Chapter 7

Shocks

7.1 What are shocks, and why do they occur?

In the previous Chapter we discussed the propagation of *small-amplitude* disturbances, and showed that they take the form of linear waves. It was easy to find wave solutions by using the fluid equations in the linearized version, which neglects the non-linearities stemming from terms like $(\boldsymbol{V} \cdot \boldsymbol{\nabla})\boldsymbol{V}$ in the equation of motion. In this Chapter I will condider the opposite limit of *strong* disturbances, where the fluid properties change rapidly. In this case the *intrinsic non-linearity* of the fluid equations plays an essential role. In particular I will discuss sudden transitions: shock waves and contact discontinuities which, in the limit of an ideal fluid, are infinitesimally thin.

Shock waves occur *supersonic* flows where the flow velocity exceeds the (adiabatic) sound speed. In a shock material flows across the discontinuity surface. A different type of discontinuity is the so-called *contact discontinuity* that can occur at any flow speed. A contact discontinuity is a surface separating two fluids or gases with different physical properties. Unlike a shock, there is *no* flow of mass across a contact discontinuity[1].

The simplest illustration for the reasons that lead to the formation of shock waves is a one-dimensional,isentropic (the specific entropy s is constant so that $P \propto \rho^{\gamma}$) flows[2]. Consider the equations for a one-dimensional flow in the x-direction, with a velocity $u(x\,,\,t)$, a density $\rho(x\,,\,t)$ and a pressure $P(x\,,\,t)$. The set of equations governing such a flow will be rewritten in a form that allows the identification of invariants.

[1]We neglect for the moment the effects of the thermal motion

[2]For a full discussion of the results of this paragraph see:
F.H. Shu: *The Physics of Astrophysics, Vol. II, Gas Dynamics*, University Science Books, Mill, Valley, CA, USA, Ch. 15;
L.D. Landau & E.M. Lifshitz: *Fluid Mechanics*, Course of Theoretical Physics Vol. 6, Pergamon Press, Oxford, 1959, Chapter IX

The relevant equations can be written as

$$\begin{aligned}
\frac{\partial \rho}{\partial t} + u \, \frac{\partial \rho}{\partial x} &= -\rho \left(\frac{\partial u}{\partial x} \right) \; ; \\
\frac{\partial u}{\partial t} + u \, \frac{\partial u}{\partial x} &= -\frac{1}{\rho} \left(\frac{\partial P}{\partial x} \right) \; ; \\
\frac{\partial P}{\partial t} + u \, \frac{\partial P}{\partial x} &= c_{\rm s}^2 \left(\frac{\partial \rho}{\partial t} + u \, \frac{\partial \rho}{\partial x} \right) \; .
\end{aligned} \tag{7.1.1}$$

The last equation is a simple consequence of the assumption of constant entropy,

$$P \, \rho^{-\gamma} = \text{constant}, \tag{7.1.2}$$

with the isentropic sound speed defined as before by

$$c_{\rm s}^2 = \left(\frac{\partial P}{\partial \rho} \right)_s = \frac{\gamma P}{\rho} \; . \tag{7.1.3}$$

By algebraic manipulation of these equations one can eliminate the density from these equations. By using the relation

$$\frac{{\rm d}\rho}{\rho} = \frac{2}{\gamma - 1} \, \frac{{\rm d}c_{\rm s}}{c_{\rm s}} \; , \tag{7.1.4}$$

the system reduces to a set of two partial differential equations of the form

$$\begin{aligned}
\left[\frac{\partial}{\partial t} + (u + c_{\rm s}) \, \frac{\partial}{\partial x} \right] \left(u + \frac{2}{\gamma - 1} \, c_{\rm s} \right) &= 0 \; ; \\
\left[\frac{\partial}{\partial t} + (u - c_{\rm s}) \, \frac{\partial}{\partial x} \right] \left(u - \frac{2}{\gamma - 1} \, c_{\rm s} \right) &= 0 \; .
\end{aligned} \tag{7.1.5}$$

These equations can be written in short-hand notation as

$$\mathcal{D}_+ \, \mathcal{C}_+ = 0 \quad \text{and} \quad \mathcal{D}_- \, \mathcal{C}_- = 0 \; , \tag{7.1.6}$$

where

$$\mathcal{C}_{\pm} = u \pm \frac{2}{\gamma - 1}\, c_{\rm s} \quad , \quad \mathcal{D}_{\pm} = \frac{\partial}{\partial t} + (u \pm c_{\rm s})\, \frac{\partial}{\partial x} \, . \tag{7.1.7}$$

These two equations can be interpreted as follows: the two *characteristic variables*[3] $\mathcal{C}_+$ and $\mathcal{C}_-$ are constant on curves in the $x - t$ plane which are the two trajectories defined by the (implicit) equations

$$\left(\frac{{\rm d}x}{{\rm d}t} \right)_{\pm} = u \pm c_{\rm s} \, . \tag{7.1.8}$$

These two sets of trajectories are known as the *plus-characteristic* and *minus-characteristic*. The trajectories of the plus-characteristic can be found by tracing the path in space-time $x - t$ of a hypothetical observer, which moves with a velocity equal to the sum of the *local* flow speed and the sound speed. This is exactly the speed of sound waves propagating in the same direction as the (one-dimensional) flow. In a similar fashion, the trajectory associated with the minus-characteristic has can be found by moving at a velocity equal to the speed of sound waves propagating in the direction opposite to the flow direction. This is illustrated in the figure below. These characteristic equations are true *regardless* the amplitude of the perturbations, and not just for (weak) sound waves. They have been derived using the full (non-linear) set of fluid equations.

One can prove a number of interesting general properties with the theory of characteristics, for instance:

- At any point P in the flow, only the space-time region contained between the plus- and minus characteristic originating from that point can be influenced by the physical conditions at P;
- Conversely, at any point P in the flow, only the physical conditions in the region contained within the plus- and minus characteristics *arriving* at P can influence the conditions at P

The variation of the orinary fluid variables along the characteristics can be derived directly from the isentropic gas law $P \propto \rho^{\gamma}$ and the associated relation

$$\frac{{\rm d}P}{\rho} = c_{\rm s}^2 \, \frac{{\rm d}\rho}{\rho} = \frac{2 c_{\rm s}}{\gamma - 1} \, {\rm d}c_{\rm s} \, . \tag{7.1.9}$$

[3] Usually called the **Riemann Invariants** in the context of fluid mechanics.

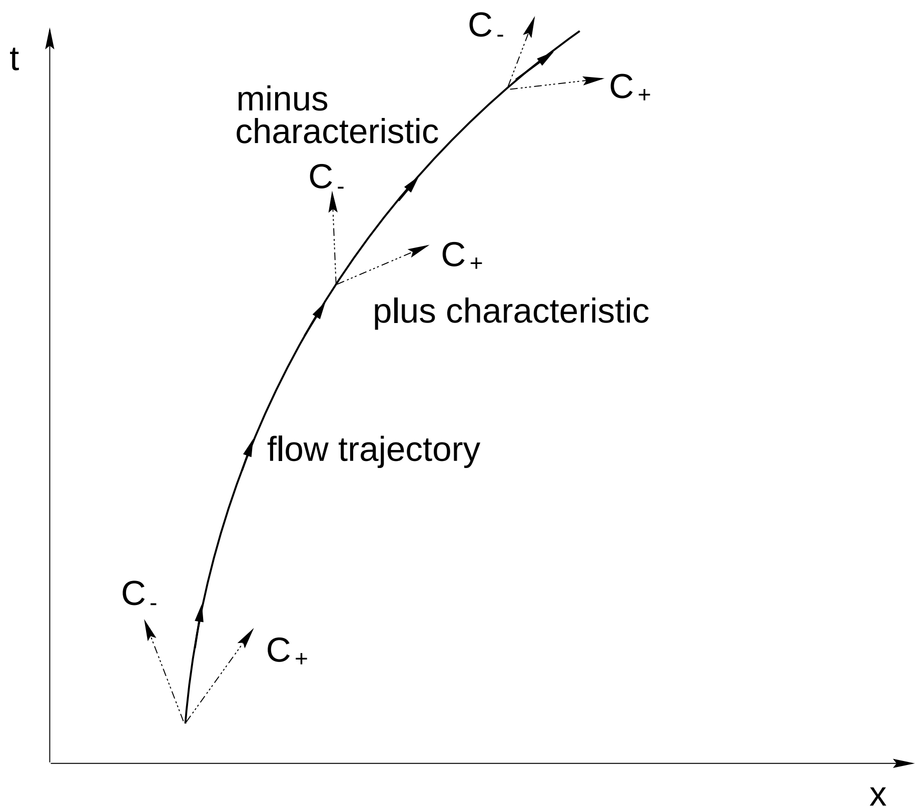

Figure 7.1: *Diagram showing the space-time flow line, defined by* $\mathrm{d}x = u\,\mathrm{d}t$*, and the two characteristics* $\mathcal{C}_+$ *and* $\mathcal{C}_-$ *defined by* $\mathrm{d}x = (u + c_\mathrm{s})\,\mathrm{d}t$ *and* $\mathrm{d}x = (u - c_\mathrm{s})\,\mathrm{d}t$*. From each point in the flow two characteristics originate along which* $\mathcal{C}_+$ *and* $\mathcal{C}_-$ *are constant respectively. Note that the value of* $\mathcal{C}_\pm$ *can be different on the different characteristics so that the characteristic variables* $\mathcal{C}_+$ *and* $\mathcal{C}_-$ *are* **not** *global constants!*

This relation allows one to write the condition that $\mathcal{C}_{\pm}$ remain constant along their respective characteristic trajectories as:

$$\mathrm{d}\mathcal{C}_{\pm} = \mathrm{d}u \pm \frac{2}{\gamma - 1}\,\mathrm{d}c_{\mathrm{s}} = 0 \quad \Longleftrightarrow \quad \mathrm{d}u \pm \frac{\mathrm{d}P}{\rho c_{\mathrm{s}}} = 0 \; . \qquad (7.1.10)$$

Here I have used Eqn. (7.1.9). This means that the two Riemann invariants $\mathcal{C}_{+}$ and $\mathcal{C}_{-}$ can also be expressed as

$$\mathcal{C}_{\pm} = u \pm \int \frac{\mathrm{d}P}{\rho c_{\mathrm{s}}} \; , \qquad (7.1.11)$$

up to an arbitrary integration constant.

7.1.1 Application to sound waves

Let us apply this to a simple small-amplitude sound wave propagating along the x-axis in the positive x-direction, with a wave vector $\boldsymbol{k} = k\,\hat{\boldsymbol{e}}_x$. In absence of the wave the fluid is at rest ($u = 0$). Using the relations (6.5.6) derived in the previous Chapter, together with the sound wave frequency that follows from the dispersion relation

$$\omega = |\boldsymbol{k}| c_{\mathrm{s}} \; , \qquad (7.1.12)$$

it is easily checked that the velocity induced by the presence of the wave equals

$$u = \delta V = \frac{\delta P}{\rho c_{\mathrm{s}}} \; . \qquad (7.1.13)$$

Here I have used that both the wave vector $\boldsymbol{k}$ and the amplitude $\boldsymbol{a}$ of the wave are along the x-axis.

Without the wave, the Riemann invariants $\mathcal{C}_{\pm}$ have constant values in the uniform, stationary gas:

$$\mathcal{C}_{+}^{0} = -\mathcal{C}_{-}^{0} = 2c_{\mathrm{s}}/(\gamma - 1) \equiv \mathcal{C}_0 \; . \qquad (7.1.14)$$

Here c_{s} is the sound speed in the unperturbed uniform gas. The presence of the small-amplitude sound wave changes the Riemann constants.

They now equal (compare Eqn. 7.1.10)

$$\mathcal{C}_{\pm} = \pm\mathcal{C}_0 + \delta V \pm \frac{\delta P}{\rho c_{\rm s}} \; . \tag{7.1.15}$$

It is easily seen form (7.1.13) that a forward propagating wave changes $\mathcal{C}_+$ to

$$\mathcal{C}_+ = \mathcal{C}_0 + \frac{2\delta P}{\rho c_{\rm s}} = \mathcal{C}_0 + 2c_{\rm s}\,\frac{\delta\rho}{\rho} \; . \tag{7.1.16}$$

Here I have used that $\delta P = c_{\rm s}^2\,\delta\rho$ in a sound wave. The second invariant $\mathcal{C}_-$ on the other hand remains unchanged: the term involving δV cancels the term involving δP. We conclude that the Riemann invariant with the characteristic trajectory running in the direction opposite to the propagation direction of the sound wave (the characteristic: ${\rm d}x = (u - c_{\rm s})\,{\rm d}t$) is not influenced by the wave, at least in the linear limit. Therefore $\mathcal{C}_- = -2c_{\rm s0}/(\gamma - 1)$ remains a global constant in this case. The other Riemann invariant $\mathcal{C}_+$ varies sinusoidally around $\mathcal{C}_0$ due to the presence of the sound wave, and will therefore take different values on the different plus-characteristics that originate along the wave.

As the wave propagates it **must** develop non-linearities in the long run as the underlying *exact* fluid equations are non-linear. This means that the displacement vector $\boldsymbol{\xi}(\boldsymbol{x}\,,\,t)$, $\delta\rho(\boldsymbol{x}\,,\,t)$ and $\delta P(\boldsymbol{x}\,,\,t)$ can no longer be described as simple sinusoidal variations in space and time. If one thinks in terms of a Fourier sum of waves with different frequencies and wavenumbers, this means that a monochromatic wave with a given frequency and wavenumber (related by the dispersion relation) will exite higher harmonics in the long run, and does not remain monochromatic.

The development of these non-linearities can be traced using the theory of characteristics. Let the density at the nodes of the wave where $\delta V \propto |\boldsymbol{a}| = 0$ be ρ_0, the unperturbed density, and the associated sound speed be equal to $c_{\rm s}(\rho_0) \equiv c_{\rm s0}$. The sound speed varies with density as

$$c_{\rm s}(\rho) = c_{\rm s0}\left(\frac{\rho}{\rho_0}\right)^{(\gamma-1)/2} \; . \tag{7.1.17}$$

The fact that $\mathcal{C}_-$ is a global constant implies that

$$\mathcal{C}_- = u - \frac{2c_{\rm s}}{\gamma - 1} = -\frac{2c_{\rm s0}}{\gamma - 1} \; . \tag{7.1.18}$$

Solving for the velocity u one finds that on the minus-characteristic x_- one must have:

$$u(x_-) = \frac{2c_{s0}}{\gamma - 1} \left[\left(\frac{\rho(x_-)}{\rho_0} \right)^{(\gamma-1)/2} - 1 \right] \tag{7.1.19}$$

Regions with a density surplus ($\rho > \rho_0$) have $u > 0$ and $c_s > c_{s0}$, and those with a density deficit ($\rho < \rho_0$) must have $u < 0$ and $c_s < c_{s0}$. This means that the plus characteristics $dx = (u + c_s)\,dt$ emanating from an overdense region travel at a larger velocity than average, but those emanating from a region of density deficit are traveling slower than average, as illustrated in figure 7.2. As a result, a sinusoidal wave must steepen as it propagates (see figure 7.3): the wave crests (regions with a density surplus) catch up with the wave throughs (regions with a lower than average density) and an acoustic wave will steepen into a saw-tooth form. The plus-characteristics from overdense and underdense regions must ultimately cross, leading to an unphysical situation: there can not be two different values for the variant $\mathcal{C}_+$ at the same space-time position. The same happens to the minus-characteristics. Therefore, something drastic must happen that prevents such an unphysical situation, in this case the formation of a shock. Sound waves in the absence of dissipation will steepen into compressive shocks!

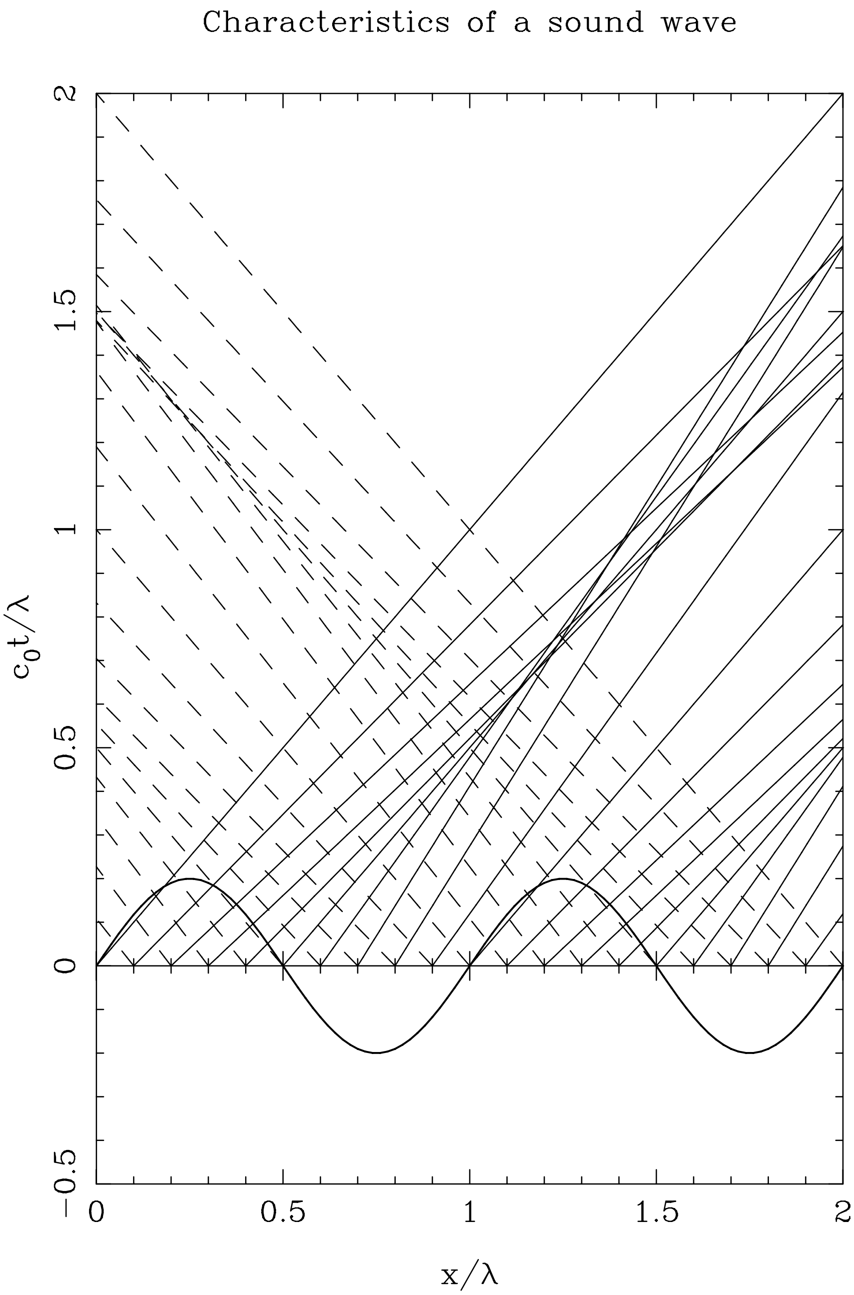

Figure 7.2: *The plus characteristics (solid lines) and minus characteristics (dashed lines) emanating from a small-amplitude sinusoidal sound wave of wavelength λ. The density amplitude of the wave is indicated (arbitrary units). The characteristics in a* **uniform** *flow with sound speed c_{s0} would correspond in this figure to lines at an inclination of ± 45 degrees with respect to the time axis. Note the crossing of the characteristics which signals that something drastic, i.e. the formation of shocks, is inevitable as the non-linearities build up.*

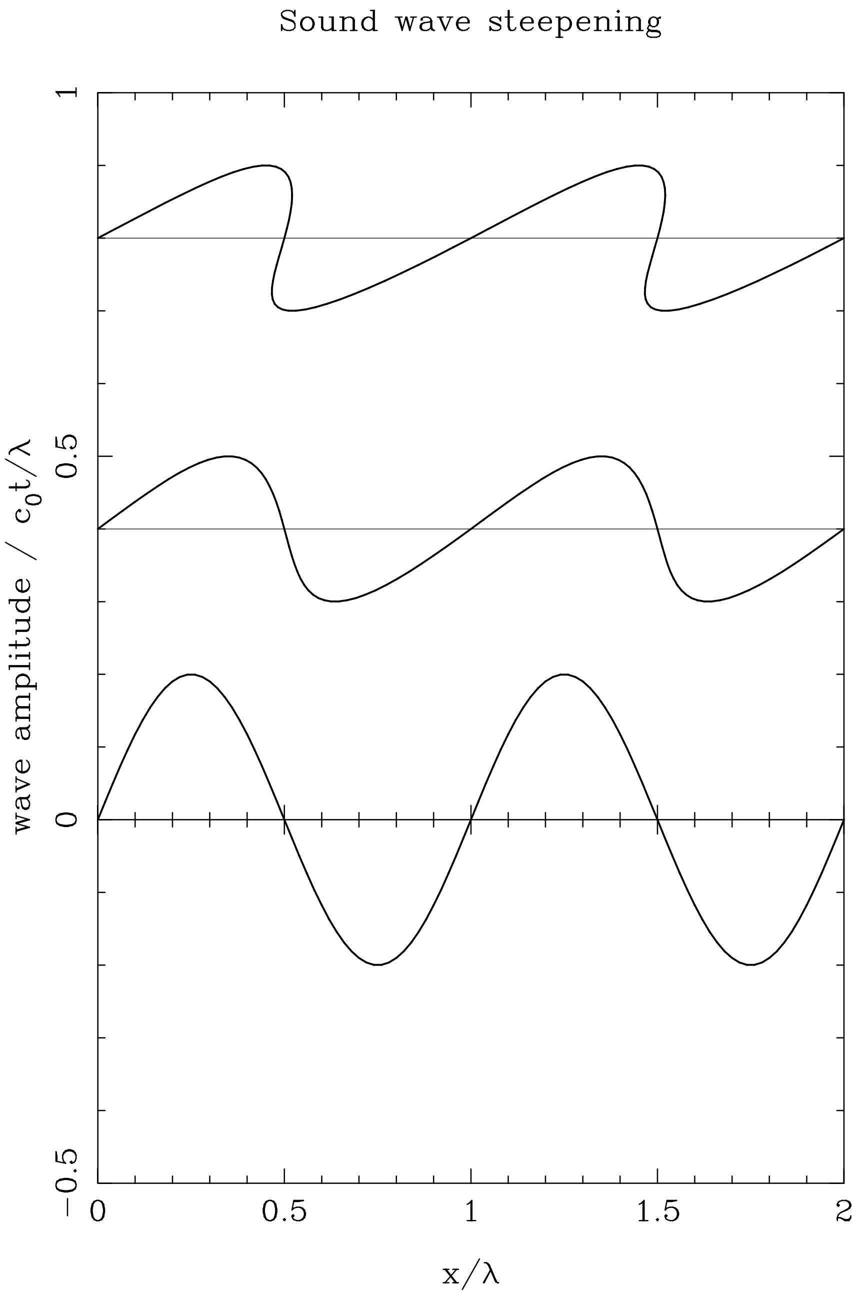

Figure 7.3: *The shape of an initially sinusoidal sound wave at* $t = 0$, $c_{s0}t/\lambda = 0.4$ *and* $c_{s0}t/\lambda = 0.8$. *The sound wave steepens. Before the plus-characteristics cross at* $c_{s0}t/\lambda = 0.4$ *it has a saw tooth-like shape. After the crossing of the characteristics at* $c_{s0}t/\lambda = 0.8$ *the shape is double-valued, and hence unphysical near the nodes at* $x/\lambda = 0.5$ *and* 1.5. *Before that, a shock will form at these nodes.*

7.2 Plane Shock waves: an introduction

Shock waves are a feature of supersonic flows with a Mach number exceeding unity:

$$\mathcal{M}_{\rm s} = \frac{|\boldsymbol{V}|}{c_{\rm s}} > 1 \; . \tag{7.2.1}$$

They occur when a supersonic flow encounters an obstacle which forces it to change its velocity. For instance: a bowshock forms around the Earth in the tenuous Solar Wind where the ionized wind material 'hits' the strongly magnetized Earth's magnetosphere.

We have seen in Chapter 6.4 that small-amplitude sound waves in a flow propagate with a velocity

$$\boldsymbol{v}_{\rm gr} = \boldsymbol{V} + c_{\rm s}\,\hat{\boldsymbol{\kappa}} \; , \tag{7.2.2}$$

with $\hat{\boldsymbol{\kappa}} = \boldsymbol{k}/|\boldsymbol{k}|$ the direction of propagation. Sound waves act as an 'messenger': they carry density and pressure fluctuations that in some sense alert the incoming flow when an obstacle is present. For low-Mach number flows ($\mathcal{M}_{\rm s} < 1$) waves can propagate against the flow, getting ahead of the obstacle.

However, in a supersonic flow with $\mathcal{M}_{\rm s} > 1$ the *net* velocity of the waves given by (7.2.2) is *always* directed downstream, and no waves can reach the flow upstream from the obstacle. In this situation a shock forms. In the shock, there is a sudden transition where the density, pressure and temperature of the flow increases. *Behind* the shock the temperature is so high that the component of the flow normal to the shock becomes *subsonic*. In that post-shock region, sound waves are once again able to communicate the presence of an obstacle to the flow so that pressure forces can deflect the flow, steering it around the obstacle. The figure below gives the Earth's bow shock as an example.

7.3 A simple mechanical model: the marble-tube

As a simple mechanical model for shock formation, consider the figure below. In a hollow (semi-infinite) tube, spherical marbles with a diameter D that are separated by a distance $L > D$ roll with velocity V. The end of the tube is plugged, forming an obstacle that prevents the marbles from continuing onward. As a result, the marbles collide inelastically, loose their velocity and accumulate in a stack at the plugged end of the tube. Far ahead of the obstacle, where the marbles still move freely, the line-density of marbles (the number of marbles per unit length) equals $n_1 = 1/L$. The density in the stack equals $n_2 = 1/D > n_1$. The density of the marbles increases when they are added to the stack.

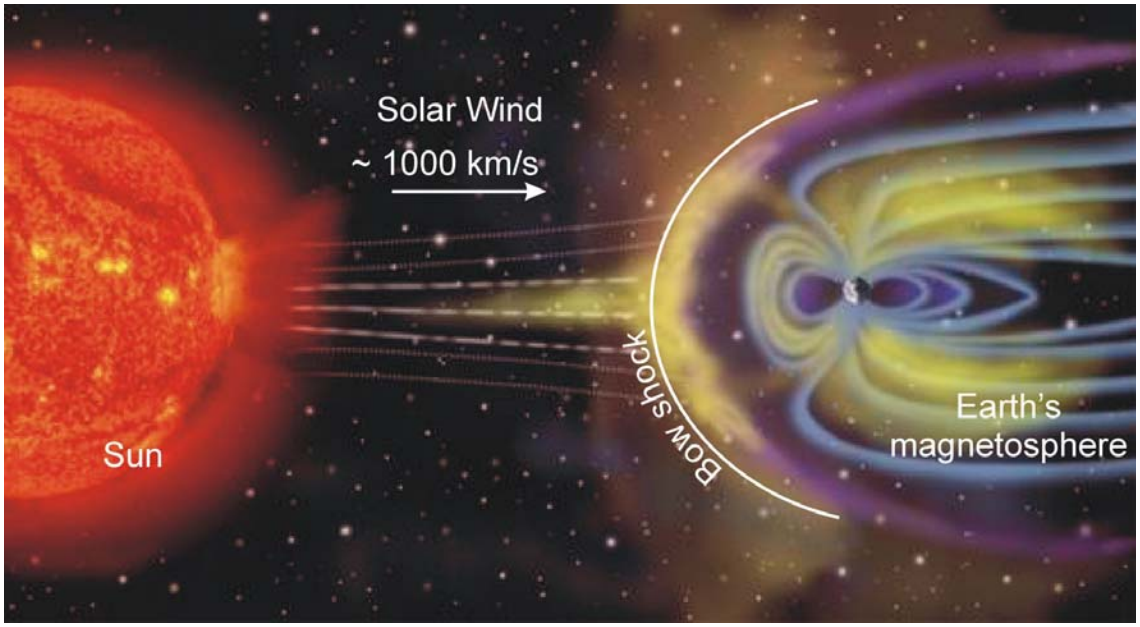

Figure 7.4: *When the Solar Wind impacts the Earth's magnetosphere, the 'sphere of influence' of the Earth's magnetic field, it forms a bow shock. In this bow shock, the incoming Solar Wind material is decelerated, compressed and heated. The properties of the Earth's bow shock can be studied using satellites*

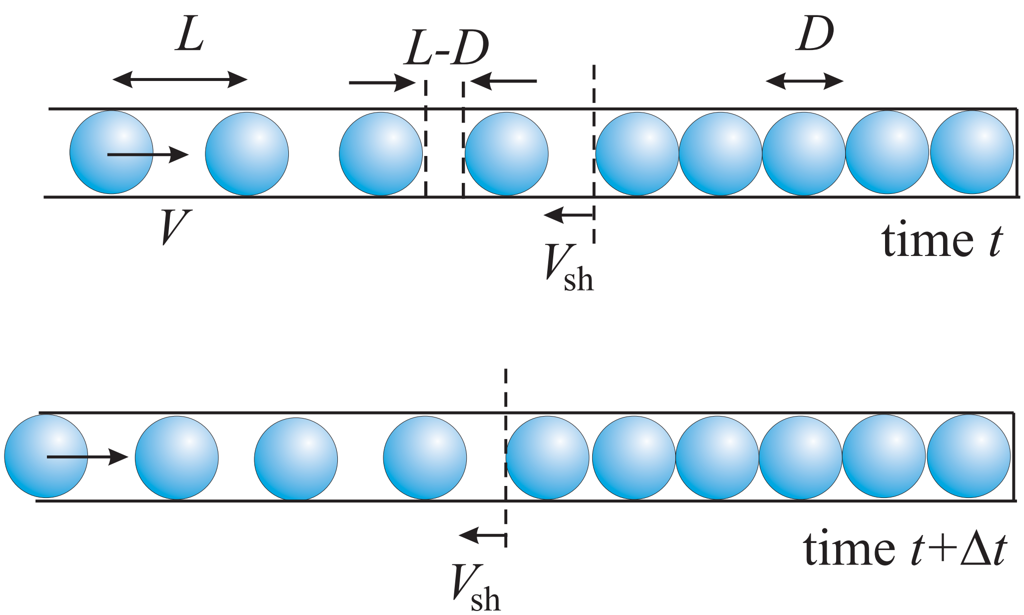

Figure 7.5: *The marble tube as a simple model of shock formation. Marbles collide at the plugged end of the tube, forming a stack that grows as time progresses. The transition between freely moving marbles, and the stationary marbles in the stack, is the analogue of a shock surface. Like a real shock, it marks the transition between a low marble density upstream, and a higher marble density downstream of the transition.*

The growth of the stack is calculated easily. In order to collide, two adjacent marbles have to close the separation distance $\Delta D = L - D$ between their surfaces. The time between two collisions at the front of the stack is therefore

$$\Delta t_{\rm coll} = \frac{L - D}{V} \; . \tag{7.3.1}$$

At every collison, one marble is added to the stack, and the length of the stack increases by D. Therefore, the *average* velocity with which the length of the stack increases equals

$$V_{\rm sh} = -\frac{D}{\Delta t_{\rm coll}} = -V \left(\frac{D}{L - D}\right) \; . \tag{7.3.2}$$

Note that this velocity is *negative*: the minus-sign is introduced because this velocity is directed towards the left. This relation defines the 'shock velocity' in this simple model. The imaginary surface at the front end of the stack, the surface that separates a region of low marble density[4] $(n_1 = 1/L)$ from the high-density region $(n_2 = 1/D)$ in the stack, is the analogue of a hydrodynamical shock.

Let us now transform to a reference frame where the 'shock' is stationary. We neglect the fact that the stack grows impulsively each time a marble is added. In this reference frame, the shock frame, the incoming marbles have a velocity

$$V_1 = V - V_{\rm sh} = V \left(1 + \frac{D}{L - D}\right) = V \left(\frac{L}{L - D}\right) \; . \tag{7.3.3}$$

The marbles in the stack, which are stationary in the laboratory frame, move away with speed

$$V_2 = -V_{\rm sh} = V \left(\frac{D}{L - D}\right) \tag{7.3.4}$$

in the shock frame.

In *any* frame, the *flux* $\mathcal{F}$ of marbles is their line-density $\times$ their velocity. In the shock frame the flux of incoming marbles with density $n_1 = 1/L$ equals:

$$\mathcal{F}_1 = n_1 V_1 = \frac{V}{L - D} \; . \tag{7.3.5}$$

[4] The density is here a *line density*: the number of marbles per unit length.

The flux of the marbles in the stack with density $n_2 = 1/D$ equals in the shock frame:

$$\mathcal{F}_2 = n_2 V_2 = \frac{V}{L - D} \ . \tag{7.3.6}$$

Comparing this with (7.3.5) one sees that these two fluxes are equal:

$$\mathcal{F}_1 = \mathcal{F}_2 \ . \tag{7.3.7}$$

This equality has a simple interpretation. The number of marbles crossing the shock surface in a time Δt equals $\Delta N = \mathcal{F} \, \Delta t$. Since an infinitely thin surface can not contain any marbles, as it has no volume, the number of marbles entering the surface at the front must exactly equal the number that leaves in the back:

$$\Delta N_{\rm in} = \mathcal{F}_1 \, \Delta t = \Delta N_{\rm out} = \mathcal{F}_2 \, \Delta t \ . \tag{7.3.8}$$

Equality (7.3.7) follows immediately. As we will see below, many of the concepts introduced here can be immediately transplanted to the physics of shocks in a gas. In particular we will find that the flux of mass, momentum and energy satisfy relations equivalent to (7.3.7): what enters the shock surface in the front must come out in the back.

7.4 Shock waves in a simple fluid

I will consider a simple fluid with density ρ, pressure P and which satisfies the polytropic relation

$$P = \text{constant} \times \rho^{\gamma} \tag{7.4.1}$$

on either side of the shock, but *not* with the same constant on both sides as a result of dissipation (entropy increase) in the shock. I will assume that the shock is planar, located at a fixed position the $y - z$ plane. The flow is from left-to-right so that the pre-shock flow occurs for $x < 0$, and the post-shock flow for $x > 0$ (see figure 7.6). The direction normal to the shock coincides with the direction of the x-axis. The shock-normal, a unit vector pointing into the upstream flow, will be indicated by $\hat{\boldsymbol{n}}_{\rm s}$. In this case $\hat{\boldsymbol{n}}_{\rm s} = -\hat{\boldsymbol{e}}_x$. I will use the subscripts 1 (2) to indicate the values of quantities ahead of (behind) the shock.

The assumption of a *planar* shock in the $x - z$ plane can be realized if the flow properties, such as velocity, density and pressure, depend only on the $x-$coordinate: $\partial/\partial y = \partial/\partial z = 0$. I will also assume that the velocity vector lies in the $x - z$ plane:

$$\boldsymbol{V} = V_{\rm n}\, \hat{\boldsymbol{e}}_x + V_{\rm t}\, \hat{\boldsymbol{e}}_z \, . \tag{7.4.2}$$

Here I have written $V_{\rm n}$ rather than V_x, and $V_{\rm t}$ rather than V_z, in order to stress that these two velocity components are the components of the velocity normal to the shock surface and tangential to the shock surface respectively.

Neglecting the effects of gravity and dissipation in the flow on either side of the shock, the equations describing the fluid are mass conservation, momentum conservation in the x and z-direction and conservation of energy. The set of fluid equations in conservative form (see Chapter 3) in this case reduce to:

$$\begin{aligned}
\frac{\partial \rho}{\partial t} + \frac{\partial(\rho V_{\rm n})}{\partial x} &= 0 \\
\frac{\partial(\rho V_{\rm n})}{\partial t} + \frac{\partial}{\partial x}\left[\rho\, V_{\rm n}^2 + P\right] &= 0 \\
\frac{\partial(\rho V_{\rm t})}{\partial t} + \frac{\partial}{\partial x}\left[\rho\, V_{\rm n}\, V_{\rm t}\right] &= 0 \\
\frac{\partial}{\partial t}\left[\rho\left(\frac{V^2}{2} + e\right)\right] + \frac{\partial}{\partial x}\left[\rho V_{\rm n}\left(\frac{V^2}{2} + h\right)\right] &= 0\, .
\end{aligned} \tag{7.4.3}$$

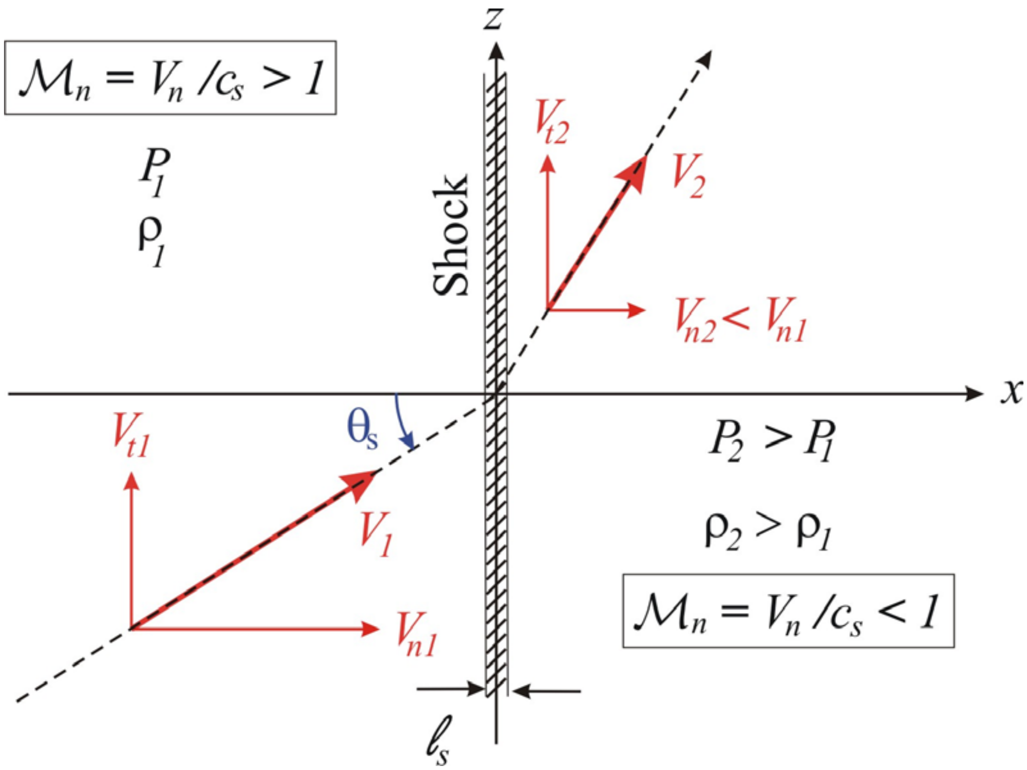

Figure 7.6: *The geometry of the flow at a planar, oblique shock. The shock is a thin transition region in the $x - z$ plane, separating the high-velocity (supersonic) incoming flow ($x < 0$) from the shocked outgoing flow ($x > 0$). Pre-shock quantities such as density and pressure are labeled with a subscript 1, and post-shock quantities with a subscript 2. The incoming flow has a velocity V_1 at an inclination angle $\theta_{\rm s}$ with respect to the direction normal to the shock surface (the x-axis). In a* normal shock *one has $\theta_{\rm s} = 0$.*
The thickness of the shock layer equals $\ell_{\rm s}$. In this Chapter, we we will take the limit of vanishing shock thickness ($\ell_{\rm s} \rightarrow 0$) in our calculations, treating the shock as a sudden jump in velocity, density and pressure.
In the shock the flow component normal to the shock is decelerated, so that $V_{\rm n2} < V_{\rm n1}$. The tangential velocity component is unchanged: $V_{\rm t2} = V_{\rm t1}$. The normal Mach number of the flow changes from supersonic ($\mathcal{M}_{\rm n} = V_{\rm n}/c_{\rm s} > 1$) ahead of the shock to subsonic ($\mathcal{M}_{\rm n} = V_{\rm n}/c_{\rm s} < 1$) behind the shock.

The quantities e and h are the internal energy per unit mass and the enthalpy per unit mass which for a polytropic fluid are given by the usual relations,

$$e = \frac{P}{(\gamma - 1)\,\rho} \quad , \quad h = \frac{\gamma\, P}{(\gamma - 1)\,\rho} \, , \tag{7.4.4}$$

and

$$V^2 = V_{\rm n}^2 + V_{\rm t}^2 \; . \tag{7.4.5}$$

All these equations have the same form:

$$\frac{\partial \mathcal{Q}}{\partial t} + \frac{\partial \mathcal{F}}{\partial x} = 0 \; . \tag{7.4.6}$$

Here $\mathcal{Q}$ is some quantity like mass density, momentum density or energy density, and $\mathcal{F}$ the flux of that quantity in the $x-$direction. Let us assume that the shock has a thickness $\ell_{\rm s}$ around $x = 0$, so that it extends in the range $-\frac{1}{2}\,\ell_{\rm s} \le x \le \frac{1}{2}\,\ell_{\rm s}$. One can integrate across the shock, from $x = -\ell_{\rm s}/2$ to $x = +\ell_{\rm s}/2$. The integrated version of (7.4.6) reads:

$$\mathcal{F}_2 - \mathcal{F}_1 \equiv \Delta\mathcal{F} = -\frac{\partial}{\partial t}\left(\int_{-\ell_{\rm s}/2}^{+\ell_{\rm s}/2} {\rm d}x \; \mathcal{Q}(x, t) \right) \; . \tag{7.4.7}$$

Here $\mathcal{F}_1 \equiv \mathcal{F}(-\ell_{\rm s}/2)$ and $\mathcal{F}_2 = \mathcal{F}(+\ell_{\rm s}/2)$ are the pre- and post-shock values of the flux. If the shock thickness $\ell_{\rm s}$ is small, and if the quantity $\mathcal{Q}$ changes from an upstream value $\mathcal{Q}_1$ in front of the shock to a downstream value $\mathcal{Q}_2$ behind the shock, one can estimate the integral in (7.4.7) using the mean value of $\partial\mathcal{Q}/\partial t$:

$$-\Delta\mathcal{F} = \int_{-\ell_{\rm s}/2}^{+\ell_{\rm s}/2} {\rm d}x \; \frac{\partial \mathcal{Q}(x, t)}{\partial t} \approx \frac{\ell_{\rm s}}{2} \left[\frac{\partial \mathcal{Q}_2}{\partial t} + \frac{\partial \mathcal{Q}_1}{\partial t} \right] \; . \tag{7.4.8}$$

If one now assumes that the shock is infinitely thin, in effect taking the limit $\ell_{\rm s} \to 0$, the integral becomes vanishingly small, $\Delta\mathcal{F} = 0$. In that case the shock is a *discontinuity surface* where the fluid properties change abruptly. Integral relation (7.4.7) in that case reduces to the conservation of flux across the shock:

$$\mathcal{F}_2 = \mathcal{F}_1 \; . \tag{7.4.9}$$

This expresses the simple fact that one can not store anything in a infinitely thin surface: there is no volume to store it in. Therefore, the principle 'flux in = flux out' must hold. Exactly the same condition was derived in the marble tube analogy for shock formation treated in the preceding Section.

Let us apply this result to the set of equations (7.4.3), which are the conservation laws for the different fluxes in the problem: the mass flux, the momentum flux that has two components, and the energy flux. For each of these four fluxes condition (7.4.9) holds. As we will see, these flux conservation laws give us the information needed to calculate the state of the gas behind the shock, given its state just ahead of the shock.

Together, the set of four equations (7.4.3) gives the following four flux conservation laws across an infinitely thin shock, the so-called **Rankine-Hugoniot jump conditions**:

$$\begin{aligned}
\rho_1 V_{\rm n1} &= \rho_2 V_{\rm n2} \equiv J \\
\left[\rho\, V_{\rm n}^2 + P\right]_1 &= \left[\rho\, V_{\rm n}^2 + P\right]_2 \\
\left[\rho V_{\rm n} V_{\rm t}\right]_1 &= \left[\rho V_{\rm n} V_{\rm t}\right]_2 \\
\rho_1 V_{\rm n1} \left[\frac{V^2}{2} + h\right]_1 &= \rho_2 V_{\rm n2} \left[\frac{V^2}{2} + h\right]_2
\end{aligned} \qquad (7.4.10)$$

The first equation states that the mass flux across the shock, $J = \rho V_{\rm n}$, is constant: you can not 'store' mass in an infinitely thin surface. Since the flow is compressed in the flow (see below, or consider the marble tube analogy) one has $\rho_2 \geq \rho_1$ and

$$V_{\rm n2} = \left(\frac{\rho_1}{\rho_2}\right) V_{\rm n1} \leq V_{\rm n1} \; . \qquad (7.4.11)$$

The second equation is the conservation of the $x-$component of the momentum flux.

The third equation is the conservation of $y-$momentum flux. Because the mass flux $J = \rho V_{\rm n} \neq 0$ does not change across the shock, the conservation of the flux of y-momentum reduces to:

$$V_{\rm t1} = V_{\rm t2} \; . \tag{7.4.12}$$

The component of velocity along the shock surface remains *unchanged*. There is a simple physical reason for this result: by transforming to a frame that moves with velocity $V_{\rm t1}$ along the z-axis towards positive z, you can transform away the perpendicular component of the velocity in the incoming flow. The shock now is a *normal shock*, with the pre-shock flow velocity along the shock normal. (In the laboratory frame, in which we performed the original calculations, the shock is an *oblique shock* provided of course that $V_{\rm t} \neq 0$.) Momentum flux conservation in the new frame of reference then tells you that the post-shock flow must *also* be in the direction normal to the shock, i.e. along the x-axis.

The conclusion of this line of reasoning is as follows: every oblique shock can be tranformed into a normal shock by choosing a new reference frame, and *vice versa* every normal shock can be transformed into an oblique shock. This implies that relation (7.4.12) must be valid.

The two relations (7.4.11) and (7.4.12) together imply that the shock refracts the flow away from the shock normal, see Figure (7.6). The angle between the velocity vector and the normal direction increases as the flow crosses the shock.

The fourth equation gives the conservation of the energy flux across the shock: Since $\rho \, V_{\rm n} = J$ does not change across the shock, this condition is equivalent with

$$\left[\frac{V^2}{2} + h \right]_1 = \left[\frac{V^2}{2} + h \right]_2 \; . \tag{7.4.13}$$

This is essentially Bernouilli's law applied to a shock. Relation (7.4.12) implies $V_{\rm t1}^2 = V_{\rm t2}^2$, and the above relation can also be written in a form that involves only $V_{\rm n}$, the normal component of the flow velocity:

$$\left[\frac{V_{\rm n}^2}{2} + h \right]_1 = \left[\frac{V_{\rm n}^2}{2} + h \right]_2 \; . \tag{7.4.14}$$

This form of the energy conservation law is once again the result of the fact that one can transform away the tangential velocity component $V_{\rm t}$, simply by moving along the shock surface with velocity $V_{\rm t}$.

This procedure leaves the effect of the shock on $V_{\rm n}$ unchanged, but eliminates $V_{\rm t}$ from the equations. In the new reference frame, the kinetic energy per unit mass of the flow is $V_{\rm n}^2/2$.

The conservation of the $x-$momentum flux and the energy conservation law can be written in an alternative form, using as a new variable the *specific volume*, defined as $\mathcal{V} = 1/\rho$. This is the volume that contains 1 gram (or 1 kg, depending on the mass units you use) of gas. The specific volume takes the following values on the upstream and downstream side of the shock:

$$\mathcal{V}_1 = \frac{1}{\rho_1} \quad , \quad \mathcal{V}_2 = \frac{1}{\rho_2} \, . \tag{7.4.15}$$

The conservation of $x-$momentum can be expressed in terms of $\mathcal{V}$ as

$$P_1 + J^2 \, \mathcal{V}_1 = P_2 + J^2 \, \mathcal{V}_2 \ . \tag{7.4.16}$$

In a similar fashion, the energy conservation law becomes

$$h_1 + \frac{1}{2} \, J^2 \, \mathcal{V}_1^2 = h_2 + \frac{1}{2} \, J^2 \, \mathcal{V}_2^2 \ . \tag{7.4.17}$$

The first equation yields

$$J^2 = \frac{P_2 - P_1}{\mathcal{V}_1 - \mathcal{V}_2} \ . \tag{7.4.18}$$

Expressing the specific enthalpy of an ideal gas in terms of $\mathcal{V}$,

$$h = \frac{\gamma \, P}{(\gamma - 1) \, \rho} = \frac{\gamma}{\gamma - 1} \, P \, \mathcal{V} \ , \tag{7.4.19}$$

one can write the energy flux conservation law as

$$J^2 \left(\mathcal{V}_1^2 - \mathcal{V}_2^2 \right) = \frac{2\gamma}{\gamma - 1} \, \left(P_2 \, \mathcal{V}_2 - P_1 \, \mathcal{V}_1 \right) \ . \tag{7.4.20}$$

Eliminating J^2 from this equation using (7.4.18) one finds the so-called *shock adiabat*:

$$\boxed{\frac{\gamma}{\gamma - 1}\,(P_2\,\mathcal{V}_2 - P_1\,\mathcal{V}_1) = \frac{1}{2}\,(\mathcal{V}_2 + \mathcal{V}_1)\,(P_2 - P_1)\ .} \tag{7.4.21}$$

One defines the *shock compression ratio* r as the density ratio across the shock:

$$r \equiv \frac{\rho_2}{\rho_1} = \frac{\mathcal{V}_1}{\mathcal{V}_2}\,. \tag{7.4.22}$$

Because of $J = \rho V_{\rm n} =$ constant, one also has:

$$r = \frac{V_{\rm n1}}{V_{\rm n2}}\ . \tag{7.4.23}$$

Substituting $\mathcal{V}_1 = r\,\mathcal{V}_2$ in (7.4.21), and solving for the compression ratio, one finds the following relation:

$$r = \frac{\rho_2}{\rho_1} = \frac{\dfrac{\gamma + 1}{\gamma - 1}\,P_2 + P_1}{\dfrac{\gamma + 1}{\gamma - 1}\,P_1 + P_2}\ . \tag{7.4.24}$$

The condition $\rho_2 > \rho_1$ implies that $P_2 > P_1$. Let us examine this relation in two important limits. In very weak shocks the fluid properties change only slightly across the shock. One can write

$$P_2 \approx P_1 + \Delta P \quad , \quad \rho_2 = \rho_1 + \Delta\rho\ , \tag{7.4.25}$$

where the pressure jump ΔP and density jump $\Delta\rho$ are small in the sense that $\Delta P \ll P_1$ and $\Delta\rho \ll \rho_1$. Substituting these relations into (7.4.24), and expanding the resulting equation to first order in ΔP and $\Delta\rho$, yields the following relation between the density jump and the pressure jump:

$$\Delta P = \left(\frac{\gamma P}{\rho}\right)_1 \Delta\rho = c_{\rm s1}^2\ \Delta\rho\,. \tag{7.4.26}$$

This relation between the pressure- and density jump is exactly the same as the one found in (small-amplitude) sound waves. For adiabatic sound waves in a gas where the pressure satisfies $P \propto \rho^{\gamma}$ one has

$$\Delta P = \frac{\partial P}{\partial \rho}\,\Delta\rho = c_{\rm s}^2 \Delta\rho\,. \tag{7.4.27}$$

Therefore *weak* shocks (so that $V_{\rm n1} \gtrsim c_{\rm s}$) can be considered for all intents and purposes as *strong* sound waves.

For very strong shocks on the other hand one expects a large pressure increase across the shock so that $P_2 \gg P_1$. In that case (7.4.24) yields an asymptotic value for the compression across the shock:

$$r \approx \frac{\gamma+1}{\gamma-1} \equiv r_{\rm max} \quad \text{(strong shock).} \tag{7.4.28}$$

This is the maximum possible compression rate of a shock in an ideal (polytropic) gas. For an ideal mono-atomic gas one has $\gamma = 5/3$, and $r_{\rm max} = 4$.

7.4.1 The Rankine-Hugoniot Relations

One can parametrize the strength of the shock by introducing the *normal Mach number* $\mathcal{M}_{\rm n}$, which is defined for $V_{\rm n} > 0$ as

$$\mathcal{M}_n = \left(\frac{V_{\rm n}}{c_{\rm s}}\right)_1 . \qquad (7.4.29)$$

It is the ratio of the upstream component of the flow speed along the shock normal, and the sound speed in front of the shock. Defining the inclination angle $\theta_{\rm s}$ of the incoming flow with respect to the direction of the shock normal by

$$V_{\rm n1} = V_1 \ \cos\theta_{\rm s} \ , \ \ V_{\rm t1} = V_1 \ \sin\theta_{\rm s} \ , \qquad (7.4.30)$$

one can write the normal Mach number in terms of $\mathcal{M}_{\rm s} = V_1/c_{\rm s}$ as

$$\mathcal{M}_{\rm n} = \mathcal{M}_{\rm s} \ \cos\theta_{\rm s} \ . \qquad (7.4.31)$$

One can express the compression ratio r and the pressure ratio P_2/P_1 across the shock in terms $\mathcal{M}_{\rm n}$. The resulting expresions are the so-called *Rankine-Hugoniot relations*[5]:

$$\begin{aligned} r = \frac{\rho_2}{\rho_1} &= \frac{(\gamma+1)\,\mathcal{M}_{\rm n}^2}{(\gamma-1)\,\mathcal{M}_{\rm n}^2 + 2} \ , \\ \frac{P_2}{P_1} &= 1 + \frac{2\gamma}{\gamma+1}\left(\mathcal{M}_{\rm n}^2 - 1\right) \ . \end{aligned} \qquad (7.4.32)$$

Shocks only exist for $\mathcal{M}_{\rm n} > 1$. If one puts $\mathcal{M}_{\rm n} = 1$, one finds $r = 1$ and $P_2/P_1 = 1$. In such a *infinitesimally weak* shock the flow crosses the shock surface *unchanged*: the density, pressure and velocity in the post-shock flow are equal the density, pressure and velocity in the pre-shock flow. In the limit of a *strong shock* with $\mathcal{M}_{\rm n} \to \infty$ one finds $r \to (\gamma+1)/(\gamma-1)$, and the pressure and temperature increase without bound. For instance: $P_2 \approx 2\gamma\mathcal{M}_{\rm n}^2/(\gamma+1) \to \infty$ as $\mathcal{M}_{\rm n} \to \infty$.

[5]e.g. , L.D. Landau & E.M. Lifshitz: *Fluid Mechanics*, Course of Theoretical Physics Vol. 6, Pergamon Press, Oxford, 1959, §85

7.5 The limit of a strong shock

In many astrophysical applications the normal Mach number is large, $\mathcal{M}_{\rm n} \gg 1$. In this *strong shock limit* the Rankine-Hugoniot jump conditions simplify considerably:

$$\begin{aligned} \frac{\rho_2}{\rho_1} &= \frac{V_{\rm n1}}{V_{\rm n2}} \approx \frac{\gamma+1}{\gamma-1} \; ; \\ \frac{P_2}{P_1} &\approx \frac{2\gamma}{\gamma+1}\,\mathcal{M}_{\rm n}^2 \; . \end{aligned} \tag{7.5.33}$$

Using the definitions (7.4.29) and (7.4.31), one finds that the post-shock pressure can be written as

$$P_2 \approx \frac{2\rho_1 V_{\rm n1}^2}{\gamma+1} = \frac{2\rho_1 V_1^2 \cos^2\theta_{\rm s}}{\gamma+1} \; . \tag{7.5.34}$$

The post-shock temperature follows from the ideal gas law, $P = \rho\mathcal{R}T/\mu$, as:

$$T_2 = \frac{\mu P_2}{\rho_2 \mathcal{R}} = \left(\frac{2\mu(\gamma-1)}{(\gamma+1)^2\mathcal{R}}\right)\,\rho_1 V_1^2\cos^2\theta_{\rm s} \; . \tag{7.5.35}$$

The sound speed in the shocked gas follows from

$$c_{\rm s2} = \sqrt{\frac{\gamma\mathcal{R}T_2}{\mu}} \approx \left(\frac{2\gamma(\gamma-1)}{(\gamma+1)^2}\right)^{1/2}\; V_1\cos\theta_{\rm s} \; . \tag{7.5.36}$$

From this it is obvious that, as an order of magnitude, one has $P_2 \sim \rho_1 V_{\rm n1}^2$ and $c_{\rm s2} \sim V_{\rm n1} = V_1\,\cos\theta_{\rm s}$. For instance: in an ideal gas with $\gamma = 5/3$ one has $P_2 = 3\rho_1 V_{\rm n1}^2/4$ and $c_{\rm s2} \approx 0.56 V_{\rm n1}$.

These (approximate) relations will be used extensively below, when we consider the physics of Supernova Remnants and Stellar Wind Bubbles that are expanding into the Interstellar Medium.

In the Box below, I will derive these relations directly from the jump conditions for the case of a normal shock.

The infinitely strong normal shock

The algebra that is involved in the solution of the general jump conditions across a shock in an ideal fluid is rather involved. There is one case, however, where the jump conditions can be solved rather simply: the *infinitely strong, normal shock*. This is the case with a vanishing pre-shock pressure, $P_1 = 0$, and with $\mathcal{M}_{\rm s} = \mathcal{M}_{\rm n} = \infty$. The jump conditions (7.4.10) reduce to the following, much simpler set of algebraic relations:

$$\begin{aligned} \rho_1 V_1 &= \rho_2 V_2 \equiv J \; ; \\ \rho_1 V_1^2 &= \rho_2 V_2^2 + P_2 \; ; \\ \tfrac{1}{2} V_1^2 &= \tfrac{1}{2} V_2^2 + \frac{\gamma P_2}{(\gamma - 1)\, \rho_2} \; . \end{aligned} \tag{7.5.37}$$

In the above set of equations I have written simply V_1 and V_2 for the pre- and post-shock flow speeds. Note that we can **not** assume that the post-shock pressure vanishes: if we put $P_2 = 0$ the only solution of this set of relations is the trivial solution: $V_1 = V_2$. There is no shock in the trivial case.

Combining the first two of these relations immediately yields:

$$V_1 - V_2 = \frac{P_2}{J} = \frac{P_2}{\rho_1 V_1} \; . \tag{7.5.38}$$

The last of the three relations of (7.5.37) can be written as

$$V_1^2 - V_2^2 = \frac{2\gamma}{\gamma - 1} \, \frac{P_2 V_2}{J} \; . \tag{7.5.39}$$

Using $V_1^2 - V_2^2 = (V_1 + V_2)(V_1 - V_2)$ and substituting for $V_1 - V_2$ from (7.5.38), this last equation can be written as:

$$\frac{P_2}{J} \, (V_1 + V_2) = \frac{2\gamma \, P_2 V_2}{(\gamma - 1)\, J} \; . \tag{7.5.40}$$

The common factor P_2/J cancels, and the resulting linear equation is easily solved for V_2 in terms of V_1:

$$V_2 = \frac{\gamma - 1}{\gamma + 1} \, V_1 \; . \tag{7.5.41}$$

Substituting this result into (7.5.38) yields the post-shock pressure:

$$P_2 = \rho_1 V_1 \; (V_1 - V_2) = \frac{2}{\gamma + 1} \, \rho_1 V_1^2 \; . \tag{7.5.42}$$

Finally, the continuity of the mass flux $J = \rho V$ gives the post-shock mass density:

$$\rho_2 = \left(\frac{V_1}{V_2} \right) \, \rho_1 = \frac{\gamma + 1}{\gamma - 1} \, \rho_1 \; . \tag{7.5.43}$$

This relatively straightforward calculation reproduces the strong-shock jump conditions that follow from the general Rankine-Hugoniot relations in the limit $\mathcal{M}_{\rm n} \rightarrow \infty$.

The case of an *oblique* infinitely strong shock with normal velocity $V_{\rm n}$ and tangential velocity $V_{\rm t}$ is easily obtained by making the replacements $V_1 \longrightarrow V_{\rm n1}$, $V_2 \longrightarrow V_{\rm n2}$ in the above expressions, and by adding the jump condition for the tangential velocity component:

$$V_{\rm t2} = V_{\rm t1} \; , \tag{7.5.44}$$

which is valid for *any* hydrodynamical shock for the reasons explained above.

7.6 Dissipation in a shock and the entropy jump

In an ideal polytropic gas the specific entropy (entropy per unit mass) is defined as

$$s = c_v \ln \left(P\rho^{-\gamma} \right) . \tag{7.6.1}$$

Since we neglected dissipation in the derivation of our equations, the specific entropy in the flow on either side of the fluid is constant:

$$s(x < 0) = \text{constant} \equiv s_1 \quad , \quad s(x > 0) = \text{constant} \equiv s_2 \; . \tag{7.6.2}$$

However, from the Rankine-Hugoniot relations (7.4.32) one can calculate s_2, given the upstream state of the gas (including s_1). If one does so one sees immediately that the $s_2 \geq s_1$ *provided* that $\rho_2 > \rho_1$ and (consequently) $P_2 > P_1$ and $V_2 < V_1$. Until now we have assumed that this is indeed the case, with the marble tube analogy as justification. The jump in the specific entropy across the shock is

$$\Delta s \equiv s_2 - s_1 = c_v \ln \left[\left(\frac{P_2}{P_1} \right) \left(\frac{\rho_1}{\rho_2} \right)^{\gamma} \right] \geq 0 \; . \tag{7.6.3}$$

One has $\Delta s = 0$ in an infinitely weak shock with $\rho_2 = \rho_1$ and $P_2 = P_1$.

In general, the entropy per particle will *increase* across the shock, a sure sign of some form of dissipation! That there must be some form of dissipation associated with the shock is intuitively obvious: part of the *kinetic* energy $\frac{1}{2}\rho_1 {V_1}^2$ of the directed motion in the upstream flow is irreversibly converted into the thermal (internal) energy of the shock-heated gas downstream. Nevertheless, the *details* of the dissipation mechanism do not enter into the final equations (the jump conditions).

In fact, one can appeal to the laws of thermodynamics in order to show that the *only* possible shock transitions are those where the density, pressure and temperature increase across the shock, and the flow velocity decreases. In that case the entropy jump is positive: $\Delta s \geq 0$. Formally, the jump conditions could also be satisfied if one interchanges the post-shock and the pre-shock flows, and where the flow velocity *increases* across the shock. That would be a transition where the density, pressure and temperature *decrease* across the shock, and where the flow accelerates rather than decelerates. In such a transition the specific entropy *decreases*: $\Delta s < 0$. Thermodynamics tells you that the entropy of the system can only stay equal or increase. $\Delta s \geq 0$. This thermodynamic law specifically *excludes* a shock transition where the flow is accelerated rather than decelerated.

One can think of a shock as a *self-regulating structure* in the following sense: the jump conditions (7.4.10), which were derived assuming an infinitely thin shock, put a strong constraint on the system: *given* the upstream state of the fluid (i.e. ρ_1, $\boldsymbol{V}_1$ and P_1) and the direction of the shock normal $\hat{\boldsymbol{n}}_{\rm s}$, the downstream state is *completely* determined by the Rankine-Hugoniot relations. The detailed (microscopic) structure of the shock, such as it's thickness, will have to adjust in such a way that the dissipation in the shock is exactly at the level required to reach a downstream state where the density, pressure and flow velocity are equal to the values that follow from the jump conditions.

The details of the dissipation only determine the thickness of the layer in which the fluid makes the transition from the upstream state to the downstream state. If the dissipation in the transition layer is due to two-body collisions between molecules or atoms, one can show that the typical thickness of the shock is of similar magnitude as the mean-free-path of the atoms or molecules in the gas. This mean free path is the typical distance an atom or molecule can travel between two collisons. The collisions convert part of the directed kinetic energy of the incoming flow into the kinetic energy of the random thermal motions of the individual atoms or molecules.

7.6.1 Shock thickness and the jump conditions

The formal derivation of the jump conditions in the preceding Sections assumes that the shock transition layer is infinitesimally thin. We derived that this implies that the flux entering the surface from upstream equals the flux exiting the surface into the downstream region. What happens if we allow the shock to have a finite thickness?

The answer to that question is contained in Eqn. (7.4.7): the flux $\mathcal{F}$ of some quantity entering the shock from upstream can only differ from the flux leaving the shock if the associated density $\mathcal{Q}$ of this quantity depends *explicitly* on time:

$$\frac{\partial \mathcal{Q}}{\partial t} \neq 0 \; . \tag{7.6.4}$$

This means that the flow must be time-dependent! In a steady flow, where all flow quantities are independent of time, the jump conditions are also valid in the case of a finite shock thickness.

The reason is simple. Consider two infinite surfaces, with the flow lines crossing both these surfaces. In a steady flow, no mass (and no energy or momentum) can accumulate in (or drain away from) the volume contained between these two surfaces. If it did accumulate (or drain away), the amount of mass (energy, momentum) contained between the two surfaces would grow (decay) in time, and the flow would no longer be steady. This line of reasoning also holds for two surfaces, one at the front and one at the back of a shock transition layer. This implies that the principle *flux in = flux out* also holds for shocks of finite thickness in a steady flow.

7.7 An example: over- and underexpanded Jets

In Chapter 5 we discussed Jet flows: collimated streams of gas which are in pressure-equilibrium with their surroundings. What happens if there is no pressure-equilibrium? If the flow speed inside the jet is supersonic with $\mathcal{M}_{\rm s} > 1$, the attempt of the jet to re-establish pressure equilibrium with the surrounding gas leads to a series of strong shocks in the jet flow, the so-called *Mach Disks*. These Mach Disks are oriented perpendicular to the jet axis, so that these shocks are normal shocks on the jet axis, the axis of symmetry. If the internal pressure $P_{\rm i}$ inside the jet is less than the pressure $P_{\rm e}$ in the external medium, one speaks of an *overexpanded jet* as the jet material has expanded too much, resulting in a low internal pressure. The opposite case (with $P_{\rm i} > P_{\rm e}$) is called an *underexpanded jet*.

What happens in these jets is illustrated in the Figure below. The situation shown there is what typically results in the exhaust jet of a jet engine or a rocket engine. The pressure in such an exhaust is determined by the (chemical) processes ocurring inside the engine, where the fuel is burned. The Mach Disks can actually be observed, as is illustrated below for the case of the Bell X-1 rocket plane, the first plane to break the sound barrier, and for the Space Shuttle.

In an underexpanded jet, the jet material expands sideways, leading to a *expansion fan*: a region where the fluid expands, and pressure and density decrease. These expansion fans, which behave similar to an expansion wave, reflect off the boundary of the jet, and turn (upon reflection) into *compression fans*. Such compression fans steepen into oblique shock waves, and finally cause the formation of the Mach Disk. Material that crosses the Mach Disk is compressed and heated, so that behind the Mach Disk the jet is again underexpanded (and over-pressured) with respect to the surrounding gas that tries to confine the jet. This means that the sequence of events starts anew, and a whole series of expansion fans, compression fans and Mach Disks is possible.

In an overexpanded jet, one starts with a compression fan as the jet material is compressed in response to the higher pressure in the surrounding gas. A Mach Disk is formed, and the shock compression in this Mach Disk raises the jet pressure so that the jet material is now over-pressured (underexpanded) with respect to the surrounding gas. The development of the jet thereafter proceeds as sketched above for an underexpanded jet.

Some astrophysicists believe that the bright 'knots' observed in the jets associated with Active Galaxies, see for example Figure 5.3 for the case of M87, are caused by a similar mechanism. This idea is supported by simulations, which show that the characteristic 'diamond shape' pattern of oblique shocks and Mach Disks indeed occur, as illustrated in the third figure below.

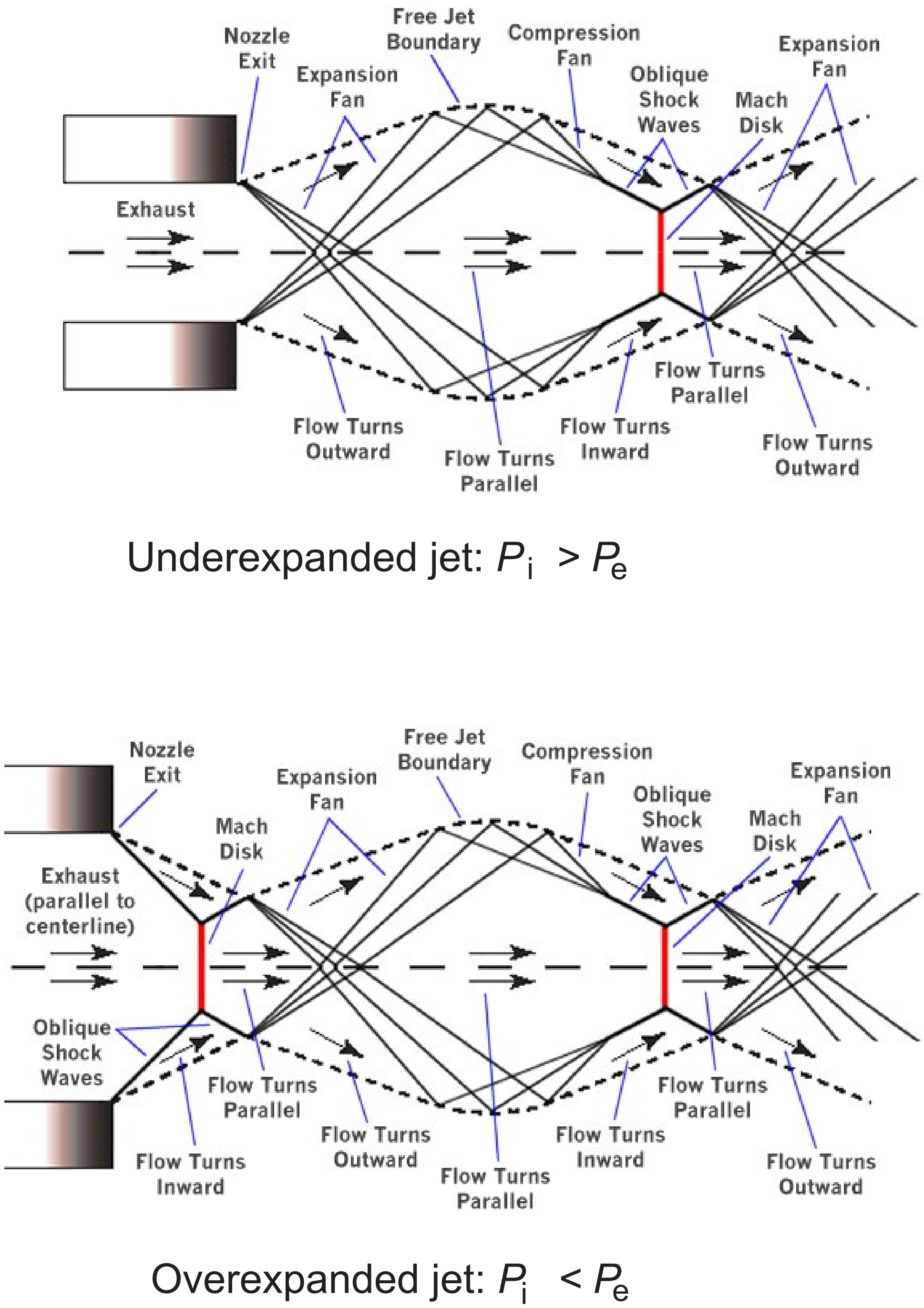

Figure 7.7: *The flow in an over- and underexpanded jet. The Mach Disks are represented by the red lines perpendicular to the jet axis.*

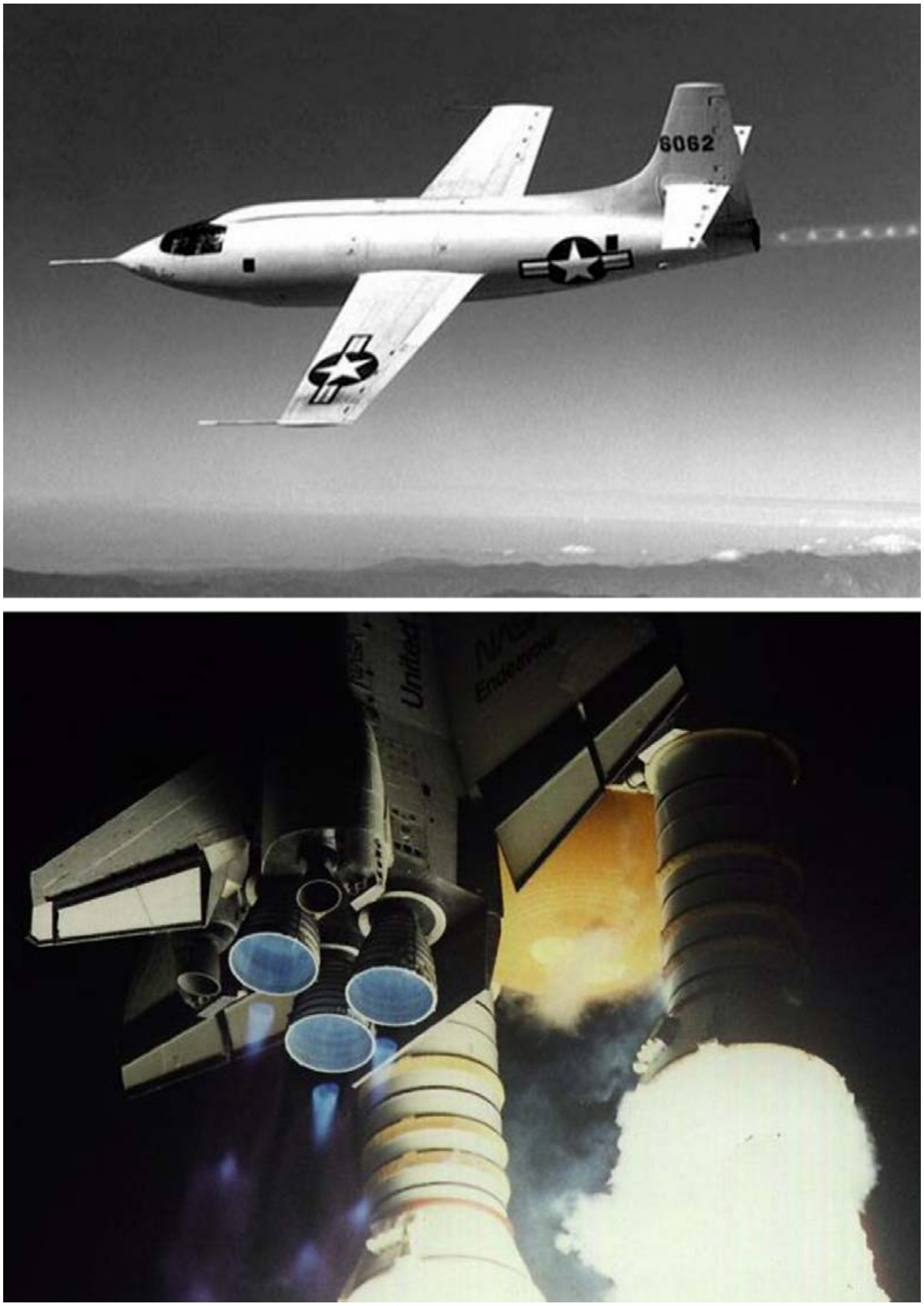

Figure 7.8: *Mach Disks in the exhaust jet of the Bell X-1 rocket plane (top), and behind the three main engines of the Space Shuttle (below). Behind the Bell X-1 a series of bright 'blobs' are visible, which show the location of the series of Mach Disks. Behind the Shuttle engines, only the first Mach Disk is clearly visible, the following disks in the series are less distinct.*

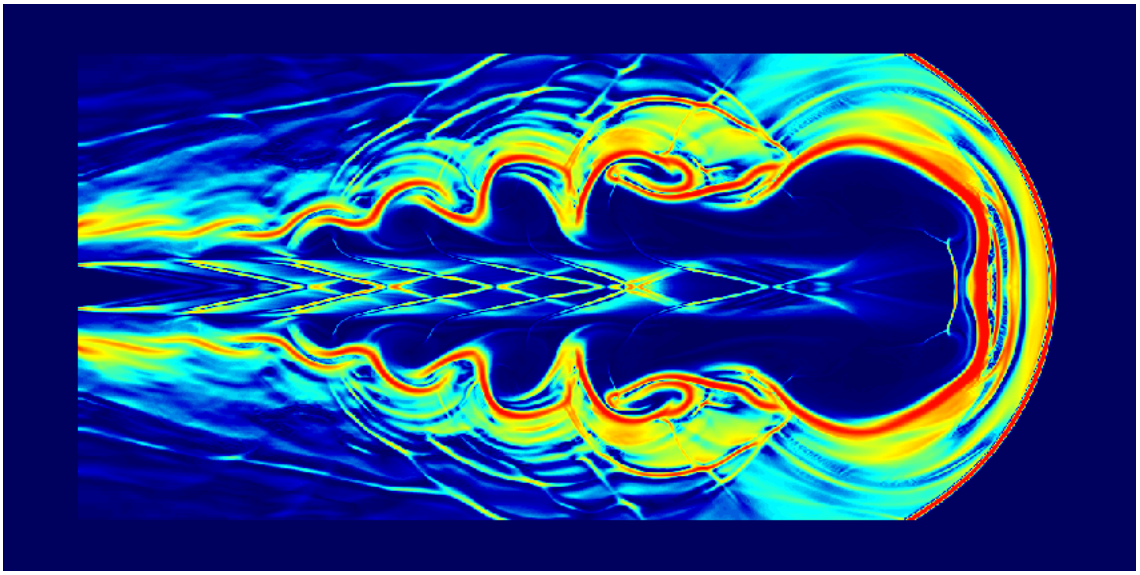

Figure 7.9: *A numerical simulation by P. Hughes, G. Comer Duncan & P. Hardee (University of Michigan) of a relativistic jet. The colors indicate different densities, with the highest densities in red, and intermediate density in yellow. Compressions are therefore colored yellow and red. Note the blunt* bow shock *preceding the jet, and the diamond-shape pattern of shocks inside the jet, just behind the head of the jet where it impacts the shocked intergalactic medium that has just passed through the bow shock. In this case, the shock diamonds are caused by the pressure fluctuations associated with the Kelvin-Helmholz Instability that occurs in the back-flow in the cocoon of shocked jet material near the head of the jet. This distorts the jet boundary and causes the wavy undulations. This instability, which occurs at a* contact discontinuity *between two fluids with a different streaming velocity, is treated in Chapter 9.*

7.8 Contact discontinuities

The jump conditions of Eqn. (7.4.10) have another solution. Let us assume that no mass crosses the discontinuity surface so that

$$V_{\rm n1} = V_{\rm n2} = 0 \; . \tag{7.8.5}$$

In that case one speaks of a *contact discontinuity*. The conservation of the flux of x-momentum, formally equal to $\rho V_{\rm n}^2 + P$, reduces to a simple pressure-balance equation:

$$P_2 = P_1 \; . \tag{7.8.6}$$

The conservation of the flux of y-momentum and the conservation of the energy flux are both satisfied trivially: both vanish identically as $\rho V_{\rm n} = 0$. This means that in a contact discontinuity the state of the fluid on both sides of the discontinuity is only constrained by the two relations (7.8.5) and (7.8.6). In particular one can have a situation where

$$\rho_2 \neq \rho_1 \; , \tag{7.8.7}$$

and the velocity, which in this case is entirely along the discontinuity surface, is unconstrained. It is not even necessary that the velocity along the contact discontinuity has the same direction on both sides. At a contact discontinuity it is allowed that

$$\boldsymbol{V}_{\rm t2} \neq \boldsymbol{V}_{\rm t1} \; . \tag{7.8.8}$$

We will see however that such a situation, where the two velocities differ across the contact discontinuity, is *unstable*: when the contact surface is warped, the deformations grow as a result of the *Kelvin-Helmholz* instability.

Summary: jump conditions at a shock

The table below summarizes the relevant relations valid at a infinitely thin shock, in the frame where the shock itself is at rest:

Definition Mach Number: $$\mathcal{M}_{\rm s} = \frac{V_1}{c_{\rm s1}} = \sqrt{\frac{\rho_1 V_1^2}{\gamma P_1}} \; ;$$

Normal Mach Number: $$\mathcal{M}_{\rm n} = \frac{V_{\rm n1}}{c_{\rm s1}} = \mathcal{M}_{\rm s} \, \cos\theta_{\rm s} \; ;$$

Density jump: $$\frac{\rho_2}{\rho_1} = \frac{(\gamma+1)\,\mathcal{M}_{\rm n}^2}{(\gamma-1)\,\mathcal{M}_{\rm n}^2 + 2} \; ;$$

Jump normal velocity: $$\frac{V_{\rm n2}}{V_{\rm n1}} = \frac{(\gamma-1)\,\mathcal{M}_{\rm n}^2 + 2}{(\gamma+1)\,\mathcal{M}_{\rm n}^2} \; ,$$

Tangential velocity: $$V_{\rm t2} = V_{\rm t1} \; ; \tag{7.8.9}$$

Pressure jump: $$\frac{P_2}{P_1} = 1 + \frac{2\gamma}{\gamma+1}\left(\mathcal{M}_{\rm n}^2 - 1\right) \; ;$$

Strong shock limit: $$\mathcal{M}_{\rm n}^2 = \frac{\rho_1 V_{\rm n1}^2}{\gamma P_1} \gg 1$$

Density jump: $$\frac{\rho_2}{\rho_1} \simeq \frac{\gamma+1}{\gamma-1} \; ;$$

Jump normal velocity: $$\frac{V_{\rm n2}}{V_{\rm n1}} \simeq \frac{\gamma-1}{\gamma+1} \; ;$$

Tangential velocity: $$V_{\rm t2} = V_{\rm t1} \; ;$$

Post-shock pressure $$P_2 \simeq \frac{2\gamma\mathcal{M}_{\rm n}^2\, P_1}{\gamma+1} = \frac{2\rho_1\, V_{\rm n1}^2}{\gamma+1} \; .$$

7.9 Supernova remnants and stellar wind bubbles

7.9.1 Blowing high-pressure bubbles into a uniform medium

In the previous Sections we considered the physics of shocks from a reference frame where the shock surface is at rest. The situation in a frame of reference where the shock moves with velocity $\boldsymbol{V}_{\rm s}$ can be obtained (for non-relativistic shock speeds) from a simple Galilean transformation. The Rankine-Hugoniot relations (7.4.32) and the jump conditions (7.4.10) can still be applied, provided one interprets the velocities V_1 and V_2 as the *relative* velocity with respect to the shock, in vector notation:

$$\boldsymbol{V} \implies \boldsymbol{V}_{\rm rel} = \boldsymbol{V} - \boldsymbol{V}_{\rm s} \, . \tag{7.9.1}$$

For a shock propagating with velocity $\boldsymbol{V}_{\rm s}$ into a medium that is at rest, $\boldsymbol{V} = 0$, one has $\boldsymbol{V}_1 = -\boldsymbol{V}_{\rm s}$ and $\theta_{\rm s} = 0$. In this particular case any shock is a normal shock, with $V_{\rm t} = 0$, even when the shock surface itself is not a plane!

Now consider a strong shock, propagating with shock speed $V_{\rm s}$ into a stationary and uniform medium with pressure $P_1 \equiv P_0$ and density $\rho_1 \equiv \rho_0$. This normal shock, with a Mach number $\mathcal{M}_{\rm n} = \mathcal{M}_{\rm s}$, satisfies:

$$\mathcal{M}_{\rm s}^2 = \left(\frac{V_{\rm s}}{c_{\rm s0}}\right)^2 = \frac{\rho_0 \, V_{\rm s}^2}{\gamma P_0} \gg 1 \, . \tag{7.9.2}$$

The strong shock limit of the Rankine-Hugoniot relations (Eqns. 7.5.33 and 7.5.34 with $\cos\theta_{\rm s} = 1$) then give the following result for the pressure P_2 immediately behind the shock:

$$\begin{aligned} P_2 &\approx \frac{2\gamma \, \mathcal{M}_{\rm s}^2}{\gamma + 1} \, P_0 \\ &= \frac{2\rho_0 \, V_{\rm s}^2}{\gamma + 1} \, , \end{aligned} \tag{7.9.3}$$

where I have used (7.9.2). One can invert this relation, and calculate the shock speed in terms of the post-shock pressure P_2, and the pre-shock density ρ_0:

$$V_{\rm s} \approx \sqrt{\frac{\gamma + 1}{2}} \, \left(\frac{P_2}{\rho_0}\right)^{1/2} \, . \tag{7.9.4}$$

This result can be applied for the formation of high-pressure bubbles in a stationary surrounding medium. This is a situation that applies to *supernova remnants* (SNRs) and *stellar wind bubbles* in the interstellar medium.

Consider a spherical bubble containing a low-density, very hot gas with internal pressure $P_{\rm i}$ and internal density $\rho_{\rm i}$. This bubble has a radius R, see the figure below. The bubble is embedded in a cold, dense stationary medium with a low pressure, $P_0 \ll P_{\rm i}$, and a high density $\rho_0 \gg \rho_{\rm i}$. Because of the large pressure difference, the bubble will start to expand rapidly. If the difference between the internal pressure $P_{\rm i}$ and the external pressure P_0 is sufficiently large, the expansion speed will be supersonic with respect to the sound speed in the surrounding medium, $\mathrm{d}R/\mathrm{d}t = V_{\rm s} > c_{\rm s0} = \sqrt{\gamma P_0/\rho_0}$. For instance, the typical (observed) expansion speed of a supernova remant is ~ 1000 km/s. The sound speed in the interstellar medium ranges from 10-100 km/s.

Because of the supersonic expansion velocity, a shock will form at the outer edge of the bubble. This shock is usually called the **blast wave**. The mass that has been swept up by the expanding bubble will collect in a dense 'shell' at its outer rim. If the shock is strong, the typical density in this shell follows from the shock jump conditions. The shocked swept-up material in the shell has a density (see Eqn. 7.5.33)

$$\rho_{\rm sh} \approx \frac{\gamma + 1}{\gamma - 1}\,\rho_0 \; . \tag{7.9.5}$$

This immediately allows us to calculate the thickness of the shell. If the external medium is uniform, a bubble with radius R has swept a total mass equal to

$$M_{\rm sw} = \frac{4\pi}{3}\,\rho_0 R^3 \; . \tag{7.9.6}$$

This mass is now residing in the dense shell with thickness ΔR and has a density $\rho_{\rm sh}$. So one must have for $\Delta R \ll R$:

$$M_{\rm sw} \approx 4\pi\,\rho_{\rm sh} R^2\,\Delta R \; . \tag{7.9.7}$$

Combining the last to equations, and using (7.9.5), one finds:

$$\Delta R = \frac{(\gamma - 1)R}{3(\gamma + 1)} = 0.083 R \; , \tag{7.9.8}$$

where the numerical value is for $\gamma = 5/3$. So the assumption that the shell is thin is a reasonable one. The swept-up material is separated from the hot material inside the bubble by a contact discontinuity.

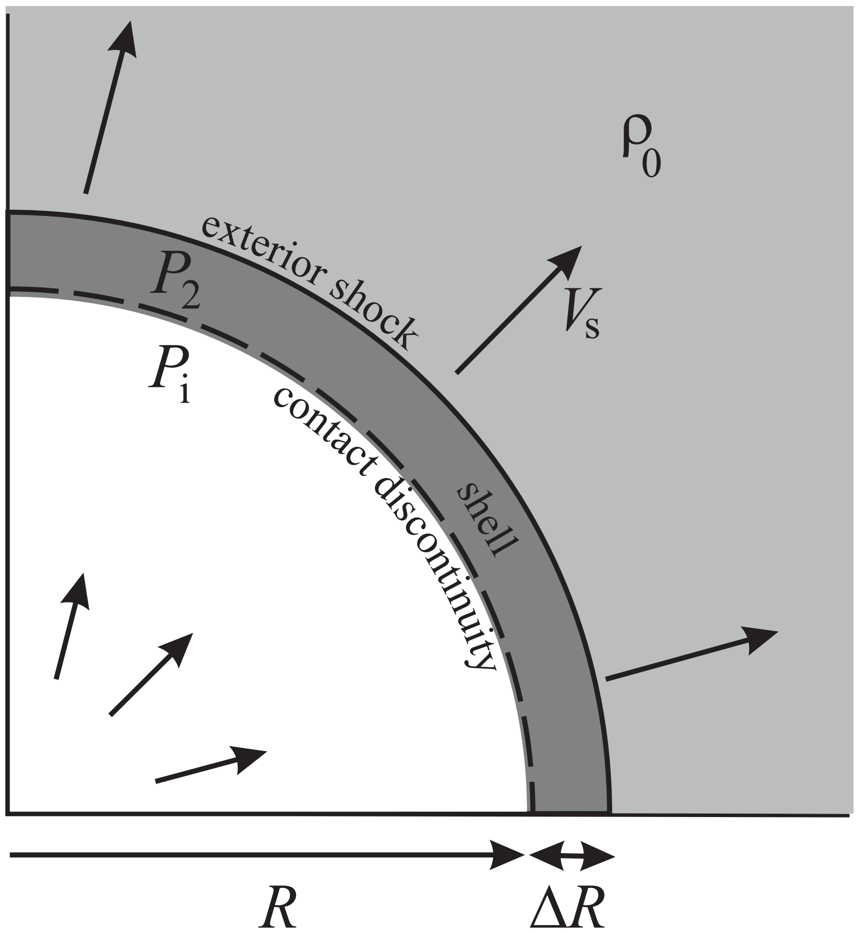

Figure 7.10: *The structure of a tenuous bubble of very hot gas (large internal pressure $P_{\rm i}$ amd small density $\rho_{\rm i}$) expanding with velocity $V_{\rm s} = {\rm d}R/{\rm d}t$ into a low-pressure, high-density medium at rest. The density of the surrounding medium equals ρ_0. If the expansion speed is supersonic with respect to the sound speed in the surrounding medium, the exterior of the bubble is a strong shock, also called a* **blast wave**. *Behind the blast wave, the material that the bubble has swept up in its life time collects in a dense shell. The hot material in the bubble interior is separated from this swept-up material by a contact discontinuity.*

The expansion speed of the bubble can be estimated from shock theory (Eqn. 7.9.4):

$$\frac{\mathrm{d}R}{\mathrm{d}t} \approx V_{\mathrm{s}} \approx \sqrt{\frac{\gamma+1}{2}} \left(\frac{P_{\mathrm{i}}}{\rho_0}\right)^{1/2} \tag{7.9.9}$$

This relation also implies that the the expansion is supersonic if $\rho_{\mathrm{i}} \ll \rho_0$: the material inside the bubble must have a very low density compared with the surrounding medium.

The associated expansion law, which gives the bubble radius $R(t)$ as a function of time, can be obtained from a simple dynamical argument. Let us assume that most of the mass of the expanding bubble is the swept-up material that has been collected over the bubble life time, and which resides in a dense shell at the outer edge the bubble with thickness $\Delta R \ll R$. This immediately gives the mass contained in the bubble as a function of the bubble radius $R(t)$:

$$M(t) \approx M_{\mathrm{sw}} = \frac{4\pi}{3}\, \rho_0\, R^3(t) \; . \tag{7.9.10}$$

The total energy of the bubble consists of the kinetic energy of the expanding massive shell, and the internal (thermal) energy of the hot, tenuous gas in the bubble interior:

$$E(t) \approx \frac{1}{2}\, M(t) \left(\frac{\mathrm{d}R}{\mathrm{d}t}\right)^2 + \left(\frac{4\pi}{3}\, R^3\right) \frac{P_{\mathrm{i}}(t)}{\gamma-1} \; . \tag{7.9.11}$$

Here it is assumed that the internal pressure is almost uniform, which is a reasonable approximation of the expansion speed is less than the *internal* sound speed:

$$V_{\mathrm{s}} \leq c_{\mathrm{si}} = \sqrt{\frac{\gamma P_{\mathrm{i}}}{\rho_{\mathrm{i}}}} \; . \tag{7.9.12}$$

In that case, the interior pressure must be roughly equal to the post-shock pressure in the shell material:

$$P_{\mathrm{i}} \approx P_2 \approx \frac{2}{\gamma+1}\, \rho_0 \left(\frac{\mathrm{d}R}{\mathrm{d}t}\right)^2 \tag{7.9.13}$$

This is simply the pressure-balance condition (7.8.6) applied at the contact discontinuity that separates the bubble interior from the shocked material in the shell. Note that (7.9.13) implies that the ratio of the thermal energy and the kinetic energy of the remnant becomes a constant (equal to $4/(\gamma^2-1) = 2.25$ for $\gamma = 5/3$) when $M(t) \approx M_{\mathrm{sw}}$.

These relations allow us to find an approximate expression for the total (kinetic + thermal) energy of the expanding, hot bubble. Substituting (7.9.13) into (7.9.11) one finds:

$$E(t) = C_\gamma \, M(t) \left(\frac{\mathrm{d}R}{\mathrm{d}t} \right)^2 . \tag{7.9.14}$$

Here C_γ is a numerical constant of order unity, which in this simple model is given by

$$C_\gamma = \frac{\gamma^2 + 3}{2(\gamma^2 - 1)} . \tag{7.9.15}$$

For an ideal mono-atomic gas with $\gamma = 5/3$ one has $C_\gamma = 1.625$. The value for C_γ is approximate, because of the various approximations made in the derivation (constant interior pressure etc.). However, more exact treatments arrive at the same result, with a somewhat smaller value for C_γ.

If one knows at which rate energy is supplied to the bubble as a function of time, so that $E(t)$ is known, one can use Eqn. (7.9.14) together with Eqn. (7.9.10) to derive the expansion law $R(t)$. We will treat two important cases: that of a point explosion where a fixed amount of energy E_0 is supplied impulsively at $t = 0$ and where no energy losses occur afterwards, so that $E(t) =$ constant $= E_0$. This is a model for a supernova remnant some 100-10,000 years after the explosion of the progenitor star. The other important case is that of a *constant* energy supply at some luminosity L so that $E(t) = Lt$. The latter case can serve as a crude model of the energy of a bubble blown into the interstellar medium by a strong stellar wind.

Another approach gives similar results. Consider the force balance of the dense shell of swept-up material. I will consider the case where of an explosive event where $E(t) = E_0$ is constant. The force balance equation can be written as a relation for the change of the shell momentum $M_{\rm sw} \, V$:

$$\frac{\mathrm{d}(M_{\rm sw} \, V)}{\mathrm{d}t} \approx 4\pi R^2 \, P_{\rm i} . \tag{7.9.16}$$

This states that the change of the magnitude of the momentum of the shell is supplied by the push excerted at its inner edge by the pressure of the hot gas inside the bubble. The assumption $P_{\rm i} \gg P_0$ allows us to neglect the force on the shell due to the pressure in the surrounding interstellar medium. If one now uses the expression $M_{\rm sw} = 4\pi\rho_0 R^3/3$, and if one estimates the internal pressure as $P_{\rm i} \sim E_0/4\pi R^3$, which assumes that about half of the total energy resides in the thermal energy in the bubble, one finds an equation of motion that will give the same expansion law as the energy argument used above.

7.10 Supernova explosions and their remnants

In a supernova the core of a massive star ($M \geq 10M_{\odot}$) which has exhausted its nuclear fuel collapses under its own weight. Without the constant energy supplied by nuclear fusion, the gas pressure drops and is no longer capable of supporting the outer layers of the star against gravity. The star starts to collapse, a collapse which proceeds most rapidly in the dense inner core. The collapse of the core continues (and accelerates) until it reaches a density comparable to that found in atomic nuclei. In that case a neutron star is left as a 'fossil' of the original exploded star. In a number of supernova remnants, such as the *Crab Nebula* (see figure) this pulsar has been detected. For a recent review about supernovae and their significance for astrophysics see Burrows[6].

The amount of energy liberated when the core collapses into a neutron star is essentially the gravitational binding energy of the core at the moment it 'bounces'. This bounce is due to the change in the equation of state of the material in the collapsing core when it is compressed to nuclear densities ($\rho \simeq \rho_{\rm nuc} = 10^{14}$ g cm^{-3}). Nuclear forces, rather than the pressure of the (degenerate) material start to dominate the pressure. With a core mass $M_{\rm c} \approx 1.5\ M_{\odot}$ and a bounce radius $R_{\rm b} \approx 10$ km (the typical mass and radius of a neutron star) the binding energy equals:

$$E_{\rm sn} \approx \frac{GM_{\rm c}^2}{R_{\rm b}} \approx 10^{53}\ {\rm erg}\ . \tag{7.10.1}$$

The binding energy is radiated away, mainly in the form of neutrinos. These neutrino's are the product of the reaction

$$p + e^- \quad \rightarrow n + \nu_{\rm e}\ , \tag{7.10.2}$$

which occurs when protons and electrons 'recombine' into neutrons within the dense, collapsing core. Neutrinos associated with the supernova SN 1987a in the Large Magellanic Cloud were detected on Earth in several experiments set up to measure proton-decay[7]. About 1 % of this energy is transferred from the neutrinos to the stellar envelope, and is used to drive a shockwave that ejects the envelope into the interstellar medium. The mechanical energy of the ejecta is therefore of order

$$E_{\rm snr} \approx 0.01 \times E_{\rm sn} \approx 10^{51}\ {\rm erg}. \tag{7.10.3}$$

This energy fuels the explosive event that ultimately creates a supernova remnant.

[6] A. Burrows, 2000: *Nature* **403**, 727.

[7] e.g.: Hirata, K *et al.*, 1987: *Phys. Rev. Lett.* **58**, 1490; Bionta, R.M. *et al.* 1987: *Phys. Rev. Lett.* **58**, 1494.

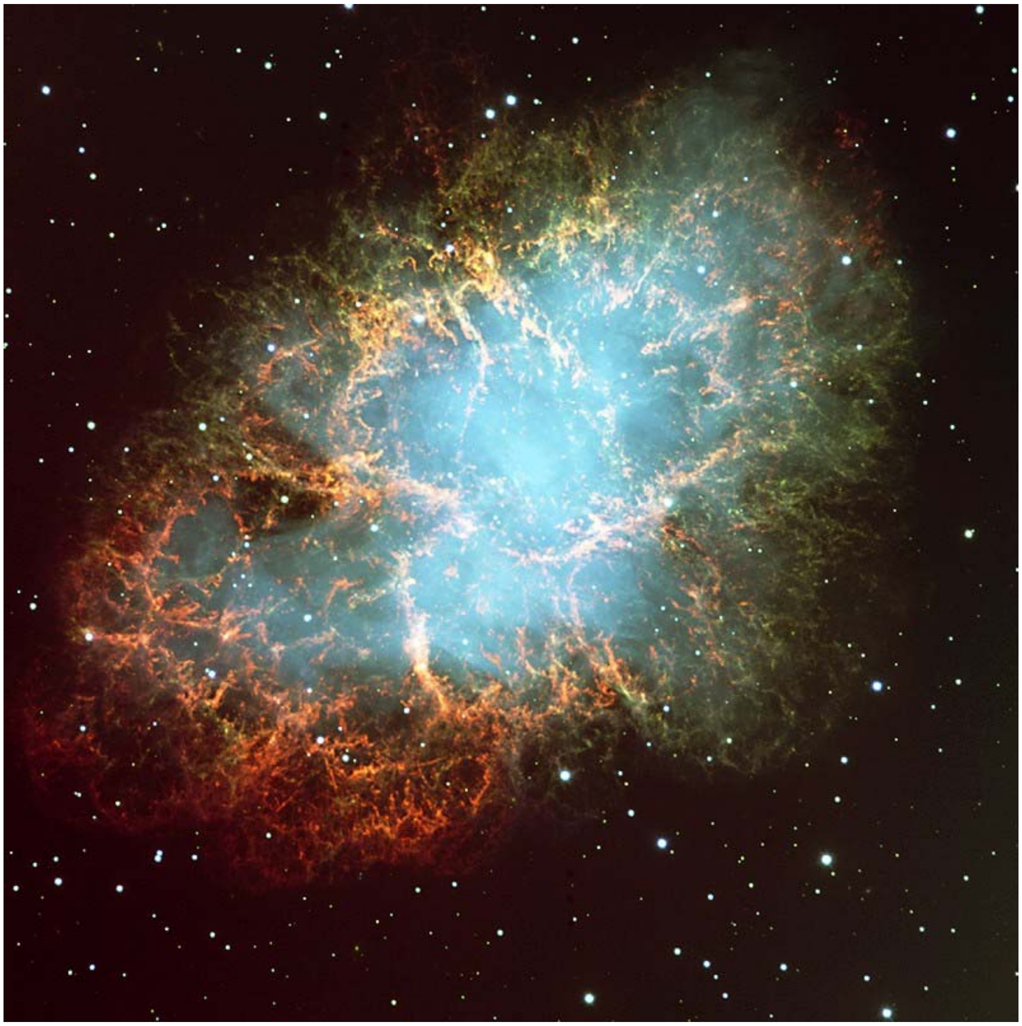

Figure 7.11: *Picture of the* Crab Nebula, *showing the optical filaments and the diffuse glow of optical synchrotron radiation due to relativistic electrons. This nebula is the remnant of the supernova of AD 1054. The actual Sedov blast wave is much larger than the structure shown here, but has as yet not been detected. This emission seen in this picture is largely powered by the* **Crab pulsar**, *the first pulsar ever discovered. This rapidly rotating neutron star spinds down slowly Apparently, most of the lost rotational energy is put into an ultra-relativistic wind. Therefore the Crab Nebula is an example of a* **pulsar wind nebula**.
Photo taken with the VLT, ESO, Chili

The whole sequence of events in a core-collapse supernova (Type II supernova in the astronomical jargon) is illustrated below.

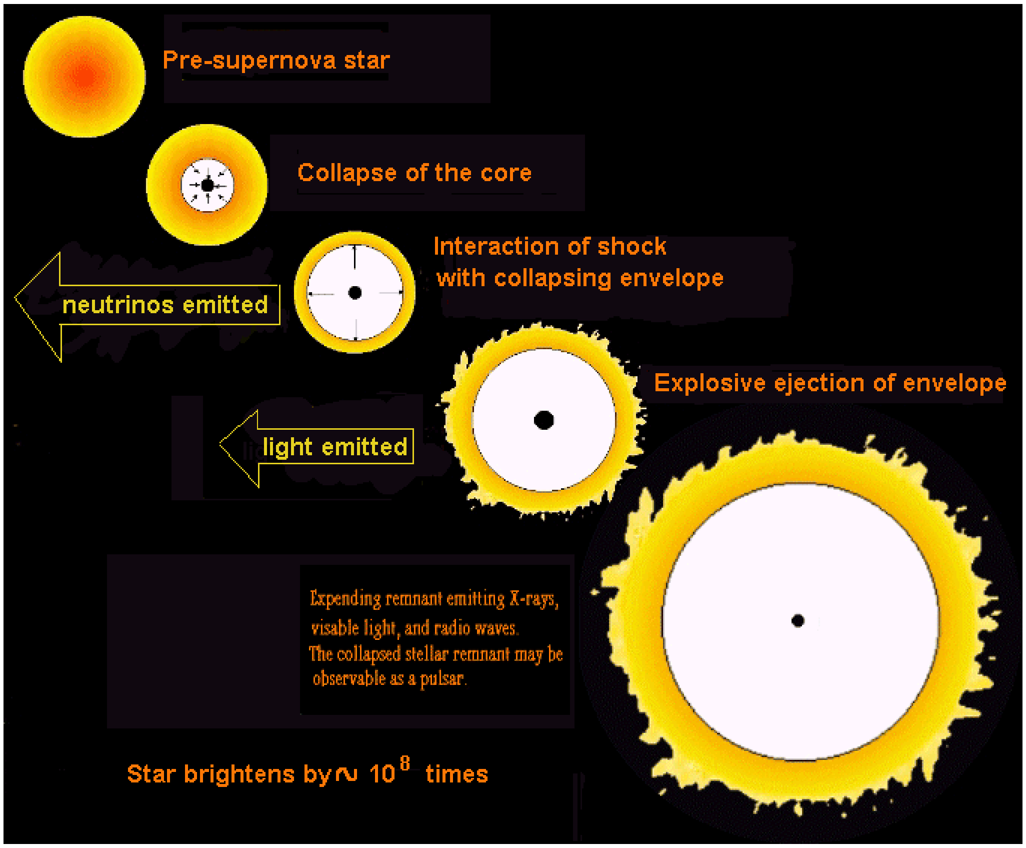

Figure 7.12: *The sequence of events leading to core collapse, and the associated supernova explosion*

A *supernova remnant* consists essentially of the stellar ejecta in a hot expanding bubble, preceded by swept-up interstellar material and an outer blast wave (strong shock) propagating into the interstellar medium. The typical speed $V_{\rm s}$ of this material can be estimated by a simple argument of energy conservation. Let us assume that all the mechanical energy is converted into the kinetic energy of the remnant, $E_{\rm snr} = \frac{1}{2} M_{\rm snr} V_{\rm s}^2$. In that case, the expansion velocity should be of order

$$V_{\rm s} \simeq \sqrt{\frac{2E_{\rm snr}}{M_{\rm snr}}} \; . \tag{7.10.4}$$

The mass $M_{\rm snr}$ is the mass of the ejecta, explosively expelled from the star at the time of the supernova explosion, and the mass $M_{\rm sw}$ (see Eqn. 8.10.10) that is added later as the remnant sweeps up more and more interstellar material.

If the density of the interstellar gas is constant and equal to $\rho_{\rm ism}$, and if the radius of the remnant is $R_{\rm s}$, one has

$$M_{\rm snr} = M_{\rm ej} + \frac{4\pi}{3}\,\rho_{\rm ism}\,R_{\rm s}^3\ . \tag{7.10.5}$$

Since we know the typical energy involved, and the mass of the remnant must be several solar masses, we can estimate the typical expansion velocity:

$$V_{\rm s} \simeq 3,000\,\left(\frac{E_{\rm snr}}{10^{51}\ {\rm erg}}\right)^{1/2}\,\left(\frac{M_{\rm snr}}{10\ M_\odot}\right)^{-1/2}\ {\rm km/s}\ . \tag{7.10.6}$$

Initially, the mass $M(t)$ of the remnant consists almost entirely of the ejecta mass, $M_{\rm ej} \simeq 2 - 10\ M_\odot$. The expansion velocity is nearly constant:

$$V_{\rm s} \simeq (2E_{\rm snr}/M_{\rm ej})^{1/2} = 10,000\ \text{km/s}. \tag{7.10.7}$$

This expansion velocity is much larger that the sound speed in the interstellar gas ($\simeq 10 - 100$ km/s), so a shock must form at the outer edge of the remnant. This phase in the evolution of the remnant is called the *free-expansion phase*.

As more and more interstellar gas is swept up, the mass of the remnant increases. After a few hundred years, the mass is dominated by this swept-up interstellar material, so that (7.10.4) reduces to:

$$V_{\rm s} \simeq \sqrt{\frac{6E_{\rm snr}}{4\pi\rho_{\rm ism}}}\,R_{\rm s}^{-3/2}\ . \tag{7.10.8}$$

The velocity decreases with increasing radius as $R^{-3/2}$ in this so-called *Sedov-Taylor phase*, the result of the increasing remnant mass: $M_{\rm snr} \propto R^3$. The typical expansion speed remains supersonic for a considerable time (typically 10,000 yr), so the shock at the outer edge of the remnant persists in this evolutionary phase.

The transition between the free expansion phase and the Sedov-Taylor phase occurs gradually when the radius of the remnant reaches the *deceleration radius* $R_{\rm d}$. The deceleration radius is defined as the radius where the ejecta mass equals the mass of the swept-up interstellar gas:

$$\frac{4\pi}{3}\rho_{\rm ism}R_{\rm d}^3 = M_{\rm ej} \iff R_{\rm d} = \left(\frac{3M_{\rm ej}}{4\pi\rho_{\rm ism}}\right)^{1/3} \simeq 2.2\left(\frac{M_{\rm ej}}{M_\odot}\right)^{1/3}\,n_{\rm ism}^{-1/3}\ \text{pc}. \tag{7.10.9}$$

Here $n_{\rm ism} \approx \rho_{\rm ism}/m_{\rm p}$ is the *number* density of the interstellar gas, which is typically $n_{\rm ism} \sim 1 \ {\rm cm}^{-3}$. It is easily checked that the relation $V_{\rm s} \propto R_{\rm s}^{-3/2}$ leads to an expansion law of the form $R_{\rm s} \propto t^{2/5}$, see below.

Later (typically after $\sim$ 10,000 years) the remnant begins to cool, and the energy is no longer conserved. The figure below gives the typical evolution of a supernova remnant, showing the free-expansion and Sedov-Taylor phase, and the following pressure-driven snowplow phase and the and momentum-conserving phases. Ultimately, a supernova remnant will merge with the general interstellar medium, leaving a Hot-Phase bubble in the interstellar medium. I will now derive the expansion law during the Sedov-Taylor phase, using the results of the previous Section.

7.10.1 The Sedov-Taylor expansion law

In a supernova explosion, the mechanical energy $E_0 \equiv E_{\rm snr}$ that drives the expansion of the bubble is supplied impulsively in a *point explosion* at time $t = 0$. If no energy is lost, for instance through radiation losses, the mechanical energy remains constant for $t > 0$. One can write the energy equation (7.9.11) in this case as:

$$E_{\rm snr} = C_{\gamma} \, M(t) \, \left(\frac{{\rm d}R}{{\rm d}t}\right)^2 = \text{constant} \tag{7.10.10}$$

The constant C_{γ} (see Eqn. 7.9.15) is of order unity. Once the remnant has expanded to a radius larger than the deceleration radius, we can use (7.9.10) for the mass of the bubble: $M(t) \approx 4\pi\rho_{\rm ism}R^3(t)/3$. The energy equation can then be written as

$$R^{3/2} \left(\frac{{\rm d}R}{{\rm d}t}\right) = \left(\frac{3E_{\rm snr}}{4\pi C_{\gamma}\rho_{\rm ism}}\right)^{1/2} = {\rm constant.} \tag{7.10.11}$$

This relationship between the velocity and the radius of the bubble, $V_{\rm s} \propto R_{\rm s}^{-3/2}$, is the same one as derived above using a simple conservation law for the kinetic energy. In this derivation we also take account of the thermal energy of the hot bubble material.

Let us try a power-law solution for the radius as a function of time:

$$R(t) = {\rm constant} \ \times \ t^{\alpha} \, . \tag{7.10.12}$$

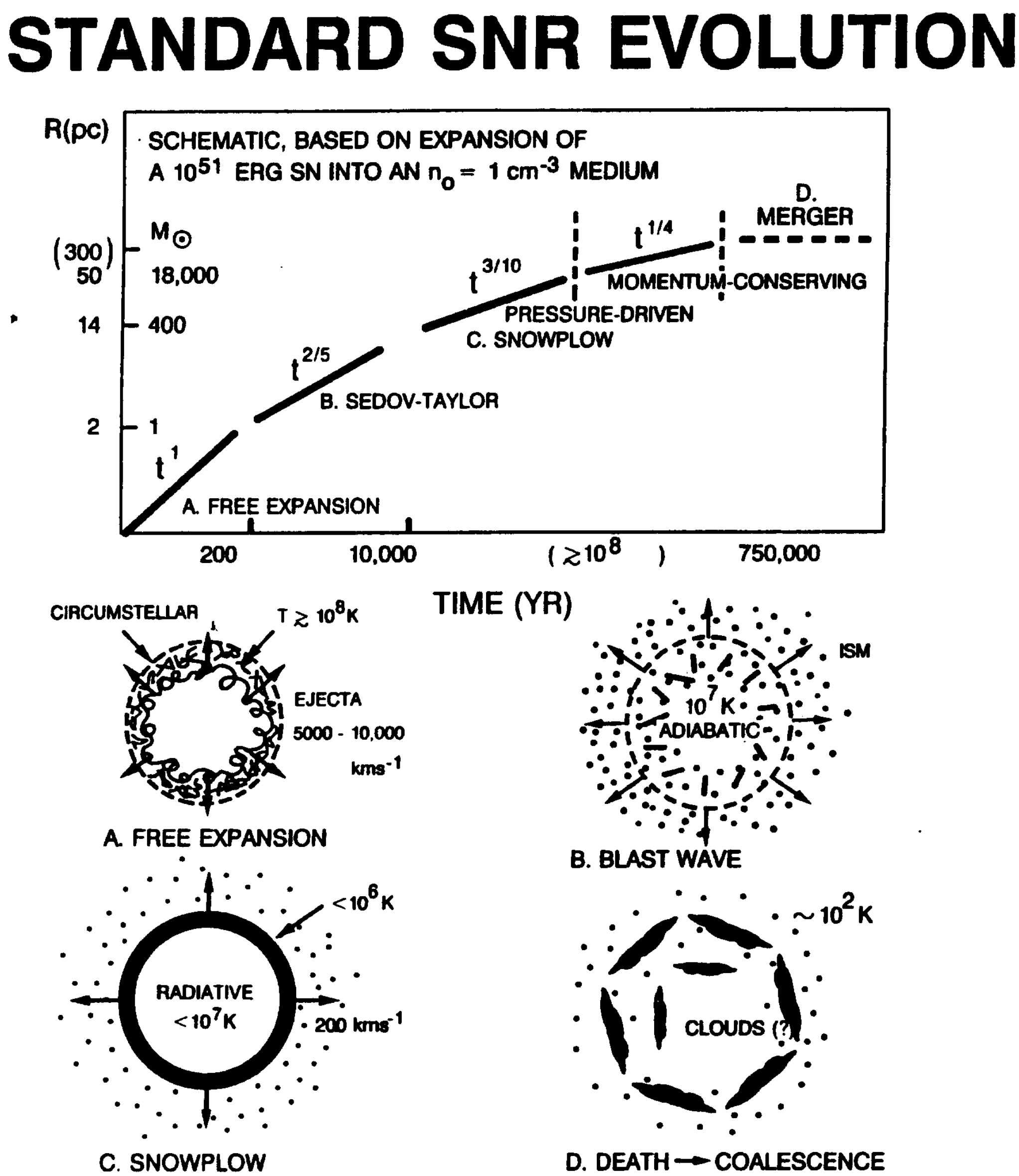

Figure 7.13: *The evolutionary stages in the life of a supernova remnant* From: Cioffi, 1990, in: *Physical Processes in Hot Cosmic Plasmas*, W. Brinkmann, A.C. Fabian & F. Giovannelli (Eds.), NATO ASI Vol. 305, p. 1, Kluwer Academic Publishers.

For an expansion law of this form the velocity is also a power-law in time:

$$V(t) = \frac{\mathrm{d}R}{\mathrm{d}t} = \alpha\,\frac{R}{t} \propto t^{\alpha-1} \tag{7.10.13}$$

Using $V = \alpha R/t$ one sees that this power law for $R(t)$ indeed solves Eqn. (7.10.11), provided that

$$\frac{R^{5/2}}{t} = \text{constant} \quad\Longleftrightarrow\quad R(t) \propto t^{2/5}\ . \tag{7.10.14}$$

This solution condition determines the power-law index as $\alpha = 2/5$. Now that the value of α has been determined one can derive the full solution:

$$R(t) = \bar{C}\,\left(\frac{E_{\rm snr}}{\rho_{\rm ism}}\right)^{1/5}\,t^{2/5} \tag{7.10.15}$$

Here $\bar{C}$ is another constant of order unity, which in our simple theory equals

$$\bar{C} = \left(\frac{75}{16\pi C_{\gamma}}\right)^{1/5} \tag{7.10.16}$$

For $\gamma = 5/3$ one finds $\bar{C} \approx 0.98$.

The pressure in the bubble decays as the bubble expands. From Eqn. (7.9.3) one has $P_{\rm i} \propto V_{\rm s}^2 \propto t^{-6/5}$. This loss of pressure is simply an expansion loss as the internal pressure is converted into the kinetic energy of the expanding shell.

This energy-conserving Sedov-Taylor solution[8] applies for $R \gg R_{\rm d}$ until the radiation losses from the remnant become important. Radiative cooling makes the pressure inside the hot bubble decay faster, and consequently the remant looses energy, and the expansion slows down more rapidly than in the Sedov-Taylor phase. The cooling-dominated stages of the remnant evolution set in after about 10,000 years.

---

[8]The Russian physicist Sedov derived this solution analytically. Sedov's method was a very clever use of a mathematical technique known as a *similarity solution*. The British physicist Taylor derived the same expansion law by numerical means. Taylor then used his model to estimate the explosive yield of the first atomic test explosions in the desert of New Mexico in 1945, using the publicly available photographs of the expanding fireball. At the time, the explosive yield of atomic bombs was considered to be classified information by the U.S.

The Sedov-Taylor solution predicts the radius and speed (shock speed) of the remnant to be

$$
\begin{aligned}
R_{\rm s} &\simeq 3.8 \left(\frac{E_{\rm snr}}{10^{51}\ {\rm erg}}\right)^{1/5} \left(\frac{n_{\rm ism}}{1\ {\rm cm}^{-3}}\right)^{-1/5} \left(\frac{t}{1000\ {\rm yr}}\right)^{2/5}\ {\rm pc} \\
V_{\rm s} &\simeq 1580 \left(\frac{E_{\rm snr}}{10^{51}\ {\rm erg}}\right)^{1/5} \left(\frac{n_{\rm ism}}{1\ {\rm cm}^{-3}}\right)^{-1/5} \left(\frac{t}{1000\ {\rm yr}}\right)^{-3/5}\ {\rm km/s}.
\end{aligned}
\tag{7.10.17}
$$

The strong shocks around the supernova remnants are believed to be the source of *cosmic rays*: a tenuous gas of very energetic charged particles (protons, electrons and nuclei) which pervades our whole galaxy. These shocks also accelerate electrons which radiate by the synchrotron mechanism in the weak magnetic field ($B \sim 10^{-4}$ G) inside the remant. This makes supernova remnants strong,non-thermal radio sources, as illustrated by the false-color picture of the radio emisson from Tycho's remnant shown below. The heated gas inside the bubble ($T \sim 10^8$ K) causes emission lines in the optical spectrum of the remant, and X-rays (thermal bremsstrahlung and atomic lines from highly ionized heavy nuclei such as Iron) which makes them also strong X-ray sources, as illustrated on the next page by the picture of Tycho's remnant in X-rays.

7.10.2 The pressure-driven and the momentum-conserving snow-plow phases

I will now briefly consider the two evolutionary phases that follow the Sedov-Taylor phase. If the supernova remnant becomes sufficiently old, radiative cooling becomes important, and the total energy is no longer conserved. In the energy conserving Sedov-Taylor phase, pressure forces accelerate the swept-up interstellar gas, converting thermal energy (which came from the original explosion) into the kinetic energy of the shell of swept-up matter. Since radiative cooling scales with the number density n as n^2, and since the density inside the shell of swept-up matter is much larger than inside the hot interior of the remnant, most of the cooling occurs in the shocked interstellar medium.

In the snow-plow approximation one assumes that all the energy put into the swept-up gas is radiated away, but that the hot interior of the remnant does not cool. This means that the shell of shocked interstellar gas collapses until it becomes very thin, and that the pressure inside the remnant now behaves adiabatically (as no heat is added to, or lost from the interior):

$$P_{\rm i} \propto \rho_{\rm i}^{\gamma} \ . \tag{7.10.18}$$

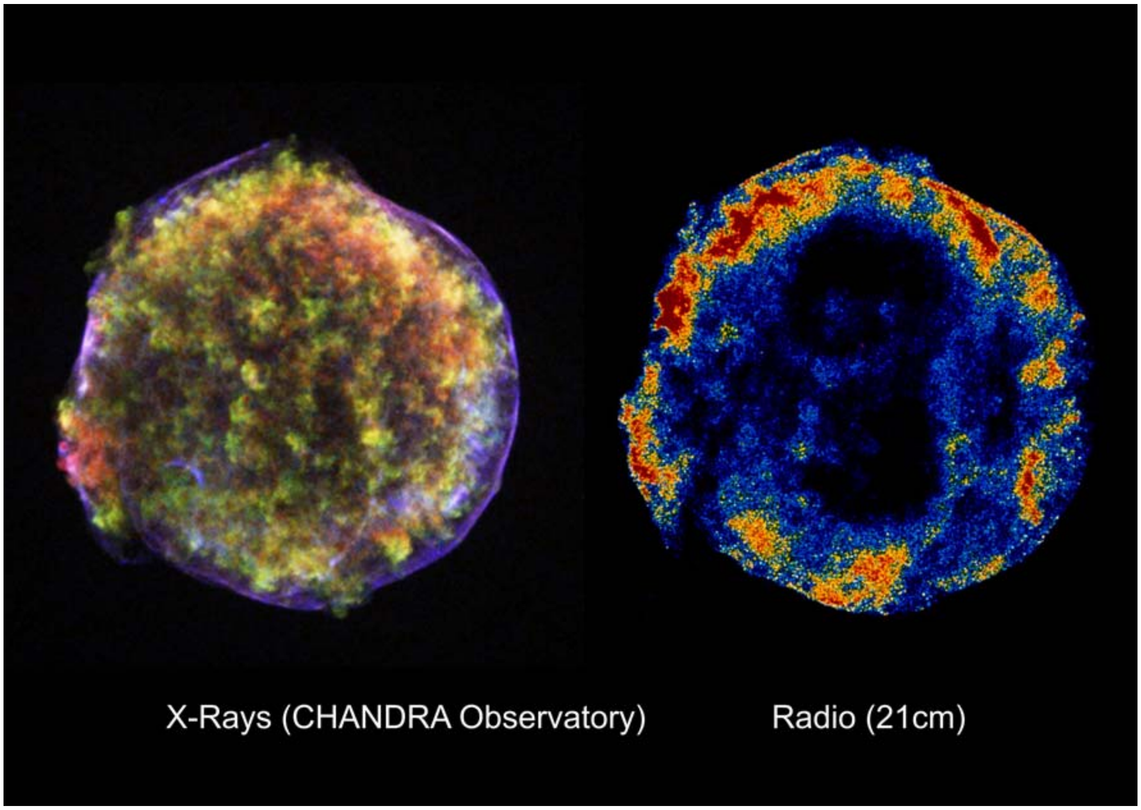

Figure 7.14: *Two pictures of the remnant of Tycho's supernova (AD 1572), a picture in X-Rays (left) , made with the CHANDRA satellite, and a radio picture made with the* Very Large Array *radio synthesis telescope (right). The X-ray picture shows the hot ($T \sim 10^8$ K) gas in the remnants interior in yellow. This is mostly* line emission *from exited nuclei. The blue radiation at the outer rim of the remnant is* synchrotron continuum emission, *caused by relativistic electrons moving in a weak magnetic field. The radio emission is also synchrotron radiation. It is believed that these relativistic electrons are accelerated at the outer shock.*
This is a 'classical' remnant with a nearly perfect spherical shape. It is believed to be entering the Sedov-Taylor phase. Note the sharp outer edge of the remnant, which is believed to coincide with the position of the outer blast wave.

Since the mass residing in the hot interior is conserved one has:

$$\rho_{\rm i} = \frac{M_{\rm ej}}{(4\pi/3)R_{\rm s}^3} \ . \tag{7.10.19}$$

Combining these two relations yields:

$$P_{\rm i} \propto R_{\rm s}^{-3\gamma} \ . \tag{7.10.20}$$

For $\gamma = 5/3$ one finds $P_{\rm i} \propto R_{\rm s}^{-5}$. This behaviour is quite different from the behaviour of the pressure in the Sedov-Taylor phase: there the pressure behaves as $P_{\rm i} \sim \rho_{\rm ism} V_{\rm s}^2 \propto R_{\rm s}^{-3}$. The motion of the collapsed shell, which contains most of the mass, is driven by the pressure of the remnant's interior. The equation of motion of the massive shell can be found by balancing the total pressure force on the shell by the inertial force,

$$\frac{{\rm d}}{{\rm d}t}\left(M(R_{\rm s})\,\frac{{\rm d}R_{\rm s}}{{\rm d}t}\right) = 4\pi R_{\rm s}^2\, P_{\rm i}(R_{\rm s}) \ . \tag{7.10.21}$$

The pressure of the interstellar medium has been neglected. Using the pressure law (7.10.20) together with $M(R_{\rm s}) = 4\pi\rho_{\rm ism}R_{\rm s}^3/3$ one finds that the equation of motion (7.10.21) can be written as:

$$\frac{{\rm d}}{{\rm d}t}\left(R_{\rm s}^3\,\frac{{\rm d}R_{\rm s}}{{\rm d}t}\right) = A\,R_{\rm s}^{2-3\gamma} \ . \tag{7.10.22}$$

Here A is a constant, whose value does not concern us here. If one tries to solve this equation with a power-law that gives the radius of the remnant as

$$R_{\rm s}(t) = B\,t^{\alpha} \tag{7.10.23}$$

with B some constant, the condition that both sides of the equation contain the same power of t gives a condition on α. It is easy to check that this condition reads

$$t^{4\alpha-2} = t^{(2-3\gamma)\alpha} \ . \tag{7.10.24}$$

Solving for α one finds:

$$\alpha = \frac{2}{3\gamma + 2} = \frac{2}{7} \approx 0.286 \; . \tag{7.10.25}$$

The last value is for $\gamma = 5/3$. So in the pressure-driven snowplow phase the supernova remnant expands as

$$R_{\rm s}(t) \propto t^{2/7} \; . \tag{7.10.26}$$

Numerical simulations of this pressure-driven snowplow phase show that the value of α is actually closer to $\alpha = 3/10 = 0.3$.

Finally, when all the internal energy of the remnant has been radiated away, the internal pressure approaches zero, and the remnant enters the *momentum-conserving snowplow phase*, where Eqn. (7.10.21) reduces for $P_i = 0$ to

$$\frac{\mathrm{d}}{\mathrm{d}t}\left(M(R_{\rm s})\,\frac{\mathrm{d}R_{\rm s}}{\mathrm{d}t}\right) = \frac{\mathrm{d}}{\mathrm{d}t}\left(M(R_{\rm s})\,V_{\rm s}\right) = 0 \iff M(R_{\rm s})\,V_{\rm s} = \text{constant} \; . \tag{7.10.27}$$

Momentum conservation yields

$$V_{\rm s}(R_{\rm s}) \propto M^{-1}(R_{\rm s}) \propto R_{\rm s}^{-3} \; , \tag{7.10.28}$$

which implies

$$R_{\rm s}(t) \propto t^{1/4} \; . \tag{7.10.29}$$

In the last stages of its life, the supernova remnant dissolves into the general interstellar medium. The figure below shows such an old remnant.

A note on using power-law solutions

I have repeatedly solved the equations of motion of a supernova remnant in different evolutionary stages with a power-law of the form $R_{\rm s}(t) \propto t^{\alpha}$. Although these are mathematically speaking perfectly good solutions, physically they are approximations simply because the assumptions behind the solutions are not valid over all time. If a supernova remnant enters a different evolutionary stage (say: it goes from the Sedov-Taylor stage to the snow plow stage) its behaviour changes, as indicated by a different expansion law. Near the time of the transition neither the Sedov-Taylor expansion law nor the pressure-driven snow plow law give a good representation of the behaviour of the remnant. The power-law solutions are only a good approximation to the exact solution if one stays well away from the point in time where the SNR changes its behaviour because the underlying physics changes!

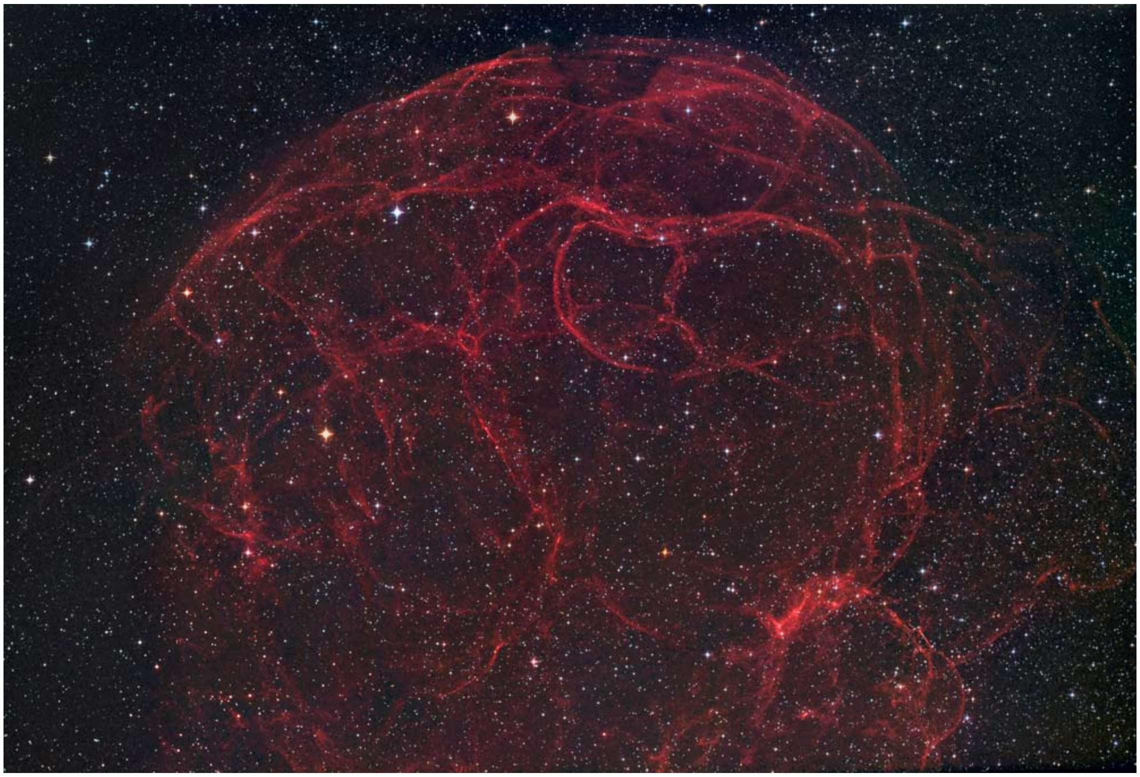

Figure 7.15: *The old supernova remnant S147, which is in the process of dissolving into the general interstellar medium.* Photo credit: Robert Gendler